

# Spatial Relationship between Precipitation and Runoff in Africa

Fidele Karamage<sup>1,2,3,4</sup>, Yuanbo Liu<sup>1</sup>, Xingwang Fan<sup>1</sup>, Meta Francis Justine<sup>2,5</sup>, Guiping Wu<sup>1</sup>, Yongwei Liu<sup>1</sup>, Han Zhou<sup>1</sup>, Ruonan Wang<sup>1</sup>

<sup>1</sup>Key Laboratory of Watershed Geographic Sciences, Nanjing Institute of Geography & Limnology, Chinese Academy of Sciences, Nanjing 210008, People's Republic of China

<sup>2</sup>University of Chinese Academy of Sciences, Beijing 100049, [People's Republic of China](#)

<sup>3</sup>University of Lay Adventists of Kigali, [Kigali](#), P.O. Box 6392, [Kigali](#), Rwanda

<sup>4</sup>Joint Research Center for Natural Resources and Environment in East Africa, [Kigali](#), P.O. Box 6392, [Kigali](#), Rwanda

<sup>5</sup>Chengdu Institute of Biology, Chinese Academy of Sciences, Chengdu 610041, People's Republic of China

10 Correspondence to: Yuanbo Liu (yblu@niglas.ac.cn [and](#), yb218@yahoo.com)

**Abstract.** Apart from the challenges of sufficient and reliable hydrological information is a key hindrance to water resource planning and management runoff prediction in Africa ungauged watersheds around different parts of the world, the direct use of river discharges on non-catchment regional studies (i.e.: country scale) also seems to be an unrealistic method that requires scientific precautions. Hence, the objective of this research is study intends to examine estimate the relationship between precipitation and runoff at three spatial scales, including the whole continent, within 25 major basins and all 55 countries. For this purpose, of the long-term monthly African continent. Initially, observed runoff coefficient ( $R_c$ ) coefficients were estimated using the long-term from monthly runoff (R) data (R) calculated from historical streamflow records provided by the Global Runoff Data Centre (GRDC) streamflow records and and monthly precipitation (P) datasets from the Global Precipitation Climatology Centre (GPCC) precipitation datasets for the period of time spanning from 1901 to 20172016. Subsequently, the observed  $R_c$  data were interpolated in order to estimate  $R_c$  over the ungauged basins under guidance of runoff coefficients for 535 catchments covering about 47.43% of the whole continent were downscaled at 0.5° grid scale based on grids' direct runoff contributions to their corresponding basins estimated following the Natural Resources Conservation Service (NRCS) runoff curve number (CN) approach. NRCS-CN involves the land use and land cover (LULC) information, soil hydrological characteristics, antecedent soil moisture condition (AMC) estimated according to an antecedent precipitation index (API) and precipitation. Predictions in ungauged basins (PUB) were achieved using the inter-gauged and ungauged basin parameter transfer method based on spatial hydrologic similarities. Monthly hydrologic similarity's feature datasets were developed from the key runoff controlling factors, including the land-AMC, CN, terrestrial water storage change (TWSC), surface temperature (T), precipitation (P) and potential runoff coefficient ( $C_p$ ) inferred from the land use and land cover, slope and topographic parameters (topographic wetness index (TWI) and soil texture information slope). The results show indicated that 4614% of the annual mean precipitation (672.52P (671.88 mm) becomes runoff (105.72 yr<sup>-1</sup>) became R (94.9 mm), with a runoff coefficient of 0.16 yr<sup>-1</sup>, and the remaining 84% (566.8086% (576.98 mm) evapotranspirates yr<sup>-1</sup>) evapotranspirated over the continent during 1901—2017. Spatial analysis reveals that the precipitation-runoff monthly and annual P-R relationship varies varied significantly among different basins and countries, mainly dependent on due to their

Formatted: Font: Times New Roman

Formatted: Font: Times New Roman, Bold

Formatted: Font: Times New Roman

climatic conditions and its inter-annual variability. Generally, high the highest runoff depths and runoff coefficients were observed over in humid tropical basins and countries/regions associated with high higher precipitation intensity intensities compared to those located in subtropical and temperate drylands.

**Keywords:** Africa; basin; evapotranspiration; GIS runoff curve number; precipitation; runoff coefficient; water balance.

## 5 1 Introduction

In the 21<sup>st</sup> century water resources management becomes a major concern to human life and environmental protection (Cosgrove and Loucks, 2015). It is well-known that precipitation is the source of freshwater on our planet, and its intensity varies from one region to another. Lacking precipitation often causes droughts which would further induces severe environment degradation, social conflicts and hunger crisis (Messer et al., 2001; Clover, 2003). Precipitation-to-runoff is the main source of water for rivers, lakes and ocean replenishment (Edwards et al., 2015). Precipitation Water scarcity aggravates poverty to an estimate of 300 million people living in the Eastern and Western drylands of Africa and the number is expected to increase by 65-80% in 2030 (Cervigni and Morris, 2016). By 2050, it is estimated that 40% of the global population will be exposed to river basins that experience severe water stress, particularly in Africa and Asia (UNISDR, 2015). On the other hand, storm water runoffs cause significant hazards and disasters such as soil erosion, floods, landslides, water pollution, and infrastructure damage (Goudie, 2000; Weng, 2001; Karamage et al., 2017a). For instance, the population exposed to flood threats Droughts further induce severe environment degradation, social conflicts and hunger crisis (Messer et al., 2001; Clover, 2003). On the other hand, intensive runoffs cause significant damages such as soil erosion, floods, landslides, water pollution, and infrastructure destructions (Goudie, 2000; Weng, 2001; Karamage et al., 2017a). For instance, the population exposed to floods increased from 0.5 to 1.8 million between 1970 and 2010 in Sub-Saharan Africa (UNISDR, 2011). Water-related problems have far-reaching effects in Africa, where, limited financial funds, sparse hydrological data and reliable scientific information bothers sustainable planning and management of water resources and related disasters (Oyebande, 2001; Karamage et al., 2016; Urroz et al., 2001).

Although runoff studies have been conducted at global scale and in some local areas in Africa (Hong et al., 2007; Fekete et al., 2002), there is no study yet indicating the spatial relationship between precipitation and runoff within all African basins and countries. In this context, current study analyzed the precipitation-runoff relationship, using an indicative runoff coefficient within 25 major basins and 55 countries in Africa. Besides, this study proposed a novel method for estimating runoff coefficient over ungauged areas based on the environmental characteristics of gauged and ungauged basins. This method derived runoff coefficient by taking consideration of its major controlling factors, which might be useful to the scientists and water resource planners. The runoff coefficient is the ratio of runoff depth to rainfall intensity within a specific watershed (Kadioglu and ŞEN, 2001) and it varies between 0 and 1 (Blume et al., 2007). It is used to indicate how much waterflow converted from precipitation within a given time and catchment. In addition, runoff coefficient is very useful for catchment

Formatted: Font: Times New Roman

Formatted: Indent: First line: 0"

Formatted: Font: Times New Roman

Formatted: English (United States)

scale land use and flood management in any catchment (Sriwongsitanon and Taesombat, 2011). Geographical Information System (GIS) has evolved since its introduction in the 1960s, and now becomes a widely used tool able to deal with multiple variables regarding basin management. However, hydrological GIS-based studies rely strongly on databases (Terakawa, 2003). In this respect, this study generated  $R_c$  based on monthly runoff calculated from the Global Runoff Data Centre (GRDC) discharges (GRDC, 2018) and Global Precipitation Climatology Centre (GPCC) precipitation products for 1901 to 2017 (Becker et al., 2013; Schamm et al., 2014) in gauged basins. The  $R_c$  data were then interpolated to the ungauged areas using the key factors such as land surface temperature (T), Precipitation (P) and potential runoff coefficient ( $C_p$ ) estimated from the land use and land cover, soil texture and slope information by using GIS spatial analysis techniques. These environmental factors are critical to the estimation of runoff coefficient (Sriwongsitanon and Taesombat, 2011; Chen et al., 2007). Impervious surfaces generally correspond to higher runoff coefficient and larger runoff volume than previous surfaces (Weng, 2001). Urbanization and cropland expansion reduces infiltration capacity and boosts the generation of surface water runoff (Goudie, 2000; Weng, 2001). Evapotranspiration is generally less than precipitation in wet seasons, that is positive water balance due to groundwater accumulation, which results in an increased surface runoff. In dry seasons evapotranspiration exceeds precipitation because the plants absorb underground water and cause a water deficit. However, underground water can be ignored in the long term annual mean water balance estimation due to a variety of wet and dry seasons (Long et al., 2014).

Geographical Information System (GIS) has evolved since its introduction in the 1960s, and now becomes a widely used tool able to deal with multiple variables regarding basin management. However, GIS-based hydrological studies rely strongly on databases (Terakawa, 2003). Various runoff-related studies have been carried out with different purposes such as, for example, runoff depth estimation at global scale (Hong et al., 2007; Fekete et al., 2002a) (Hong et al., 2007; Fekete et al., 2002b; Ruess, 2015; Smakhtin, 2004) and water stress assessment at country and global scales (Ruess, 2015; Smakhtin, 2004), modelling blue and green water availability in Africa (Schuol et al., 2008) and runoff predictions in different parts of Africa (Tesemma et al., 2010; Olang and Fürst, 2011; Jaleta et al., 2017; Mahmoud, 2014; Karamage et al., 2017a). However, based on our knowledge, there is no available detailed study on the relationship between precipitation and runoff in Africa indicating how river discharges available at catchment scale can be downscaled at small unity of land or grid scale which could be utilized reasonably to estimate P-R correlation at a non-catchment spatial scales (i.e.: countries, etc.), taking into consideration well-known key runoff controlling factors such as land use, climate, soil characteristics, etc. Briefly, this study aims at assessing the relationship between precipitation and runoff within 55 African countries and 25 major drainage basins. As scientific contribution, this study highlighted step by step how the Natural Resources Conservation Service (NRCS) runoff curve number (CN) can be a prominent proxy for the basin's river discharge downscaling at a grid scale which can be reasonably utilized on the non-catchment regional studies (i.e.: Country scale). Actually, runoff-related studies are often conducted at a drainage basin scale, but, hydrological studies on the grid and country scales are very useful at national level since each government has own policies for water resource management. For instance, it has been noticed that runoff discharges are useful in water stress analysis on country scale (Ruess, 2015; Smakhtin, 2004). Integration of NRCS-CN in downscaling the runoff discharges do not alter the quantity of observed runoff at a catchment scale, but it redistributes catchment's discharged runoff volume to its

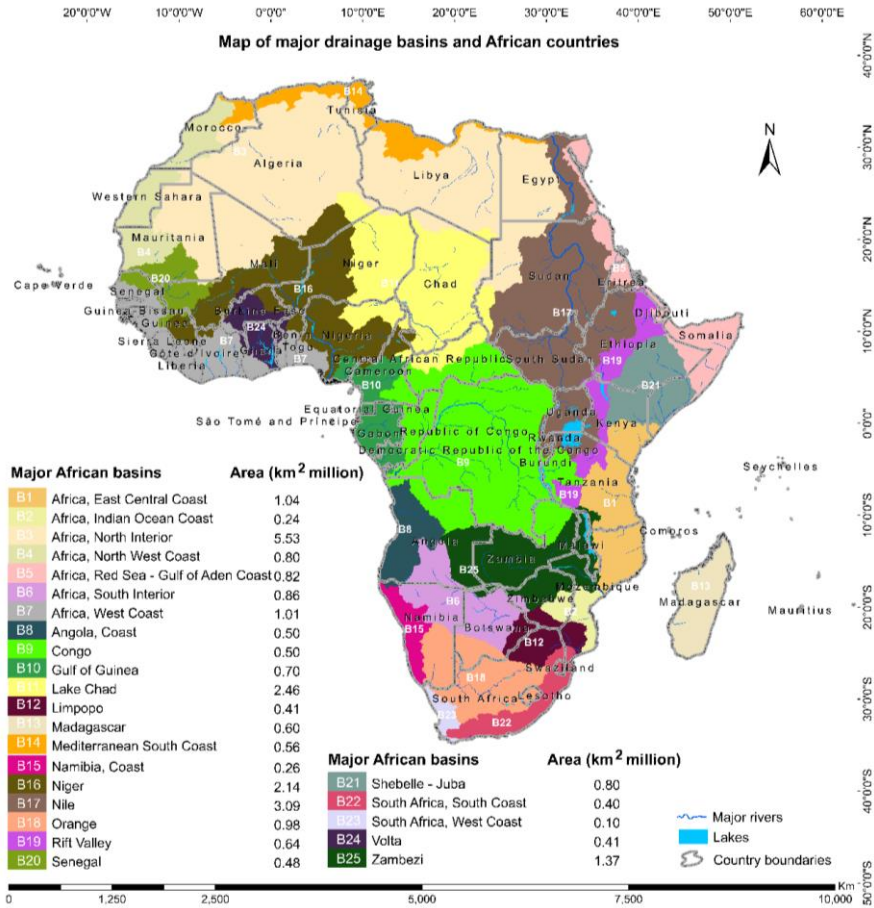
5 grids proportionally according to their respective climate and physical conditions. NRCS-CN is very useful in various hydrological studies mainly in predicting the direct runoff discharges by incorporating the land use and land cover (LULC) information, soil hydrological characteristics, antecedent soil moisture condition (AMC) and precipitation (Hawkins, 1993). Besides this, the prediction of the P-R relationship in ungauged regions was achieved utilizing the inter-gauged and ungauged basin parameter transfer method that was previously recommended in other hydrological studies as a reliable approach for parameter predictions in ungauged basins (PUB) (Bárdossy, 2007;Blöschl, 2006). Using this method, the gridded observed runoff coefficients ( $Or_c$ ) were transferred to ungauged regions according to their hydrologic similarity. Monthly hydrologic similarity's feature datasets were established from key runoff controlling factors such as: (i) AMC, (ii) NRCS-CN, (iii) terrestrial water storage change (TWSC), (iv) land-surface temperature (T), and (v) topographic parameters (topographic wetness index (TWI) and slope). The present study developed a unique monthly hydrologic similarity feature dataset with multiple zones. Each zone is composed by a set of grids with similar climatic and physical characteristics. The runoff controlling factors were firstly classified into ranges, converted to non-simplified polygons and stacked together using an overlay (intersect) analysis technique (Zhu, 2016) performed with the "intersect tool" available in "overlay tools", one of the "Analysis tools" in ArcMap v.10.5. After that, the mean observed runoff coefficients were transferred to ungauged regions employing the "Zonal Statistics as Table Tool" available in "Zonal tool" of the "Spatial Analyst Tools" in ArcMap v.10.5" where, hydrologic similarity dataset were considered as "Input raster or feature zone data", and gridded observed runoff coefficient as "Input value raster". Inter-gauged and ungauged basin parameter transfer approach was chosen to be used in this study because of its simplicity and reasonable prediction in ungauged regions, yielding the results representing a real-world phenomenon occurring in the same region. This method can be considered as one of the hybrid interpolation or gaps filling techniques which are very useful in developing various datasets such as temperature, precipitation, soil, etc.

## 2 Data inputs and Methods

### 2.1 Study area

Africa (Figure 1) is the world's second-largest continent ( $\approx 30.3$  million  $km^2$ ) accounting for 6% of Earth's surface area and 20.4 % of land area (Sayre and Pulley, 1999; Mawere, 2017). It is the second-most-populous continent (1,256 million people) after Asia (4,504 million people) as of 2017 (UN-DESA, 2017).

Formatted: Font: Times New Roman



Statistical computation from the Figure 1. Hydrological map showing major rivers, lakes, 25 major basins and 55 countries of Africa.

The European Space Agency (ESA) Climate Change Initiative (CCI) land cover (LC) map 2015 (ESA-CCI, 2017) indicated that Africa is comprised of forests (24.52%), grassland (24.51%), cropland (16.14%), built-up areas (0.16%), wetlands (0.84%), inland water (0.99%), and bare areas (32.84%).

- Formatted: Font: Times New Roman



is drained through permanent or ephemeral rivers. However, in arid areas (i.e., Northwest Sahara Desert and Somalia), drainage is sometimes absent or masked by sand seas. Approximately, 60% of the African continent is drained by 10 large rivers (Congo, Limpopo, Niger, Nile, Ogooue, Orange, Senegal, Shebelle, Volta and Zambezi) and their tributaries (Paul et al., 2014).

## 2.2 Datasets and Application

As presented by a conceptual framework (Figure 2), the goal of this study is achieved primarily using two types of data inputs (river discharge data and precipitation) in monitored basins and further auxiliary datasets comprising the land surface temperature, precipitation and potential runoff coefficient established based on the land use and land cover (LULC) maps, Digital Elevation Model (DEM) and soil properties employed to improve the interpolation accuracy of observed runoff coefficient ( $R_c$ ). The data are processed and analyzed. The data were processed and analysed using the Esri ArcGIS software version 10.5, SDMToolbox version 2.2 (Brown et al., 2017) and Excel VBA (Visual Basic for Applications) (Walkenbach, 2010). Figure 2 demonstrates the conceptual framework used to analyze the relationship between precipitation and runoff in Africa.

Formatted: Font: Times New Roman

Formatted: Font: Times New Roman

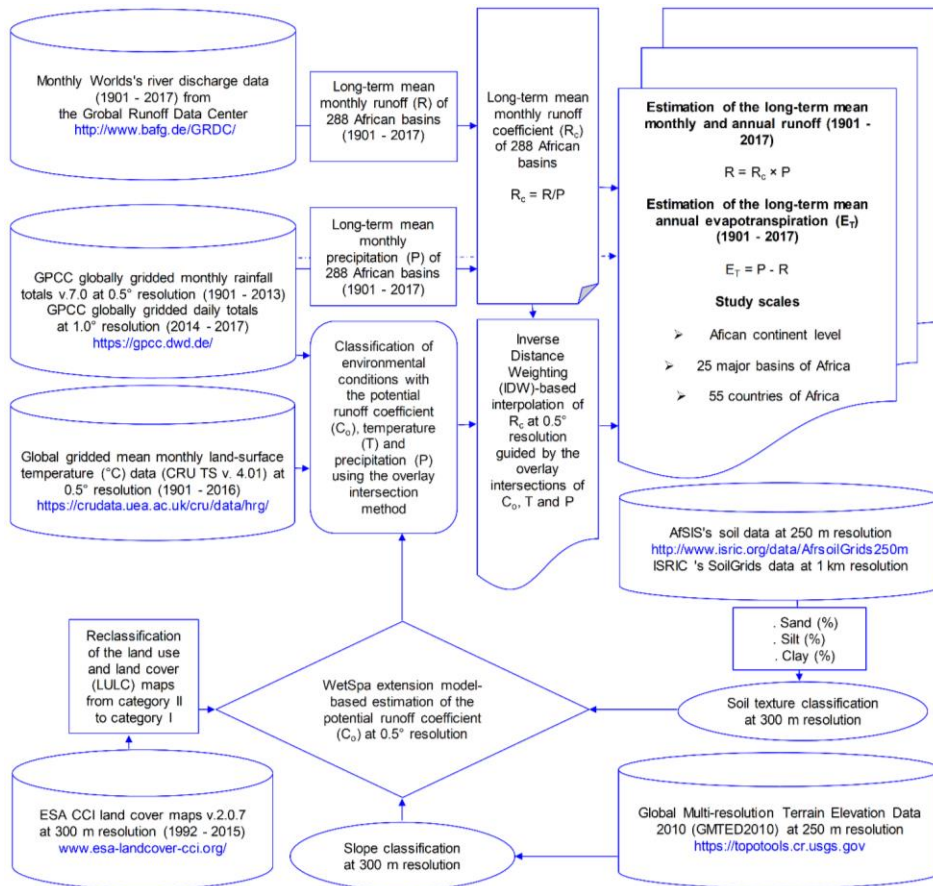
Formatted: Font: Times New Roman

Formatted: Font: Times New Roman, English (United States)

Formatted: Font: Times New Roman

Formatted: Indent: First line: 0"

Formatted: Font: Times New Roman



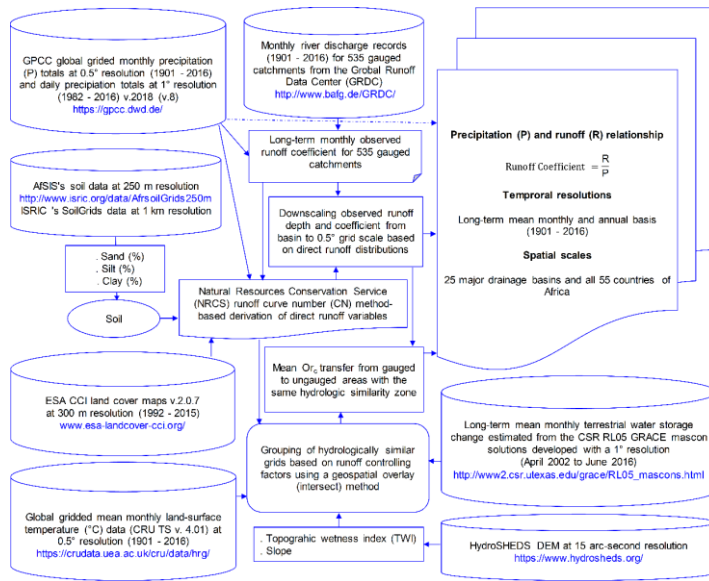


Figure 2. A conceptual framework used for analyzing the precipitation-runoff relationship in Africa.

### 2.2.1 Runoff coefficient estimation in gauged basins/catchments

The runoff coefficient in monitored basins is coefficients over gauged catchments were estimated from with two types of data: (1) the monthly time series of river discharge data for 341535 African river basins (catchments (Figure 3) discontinuously recorded since 1901 —2017) until 2016 were provided by request from the Global Runoff Data Centre (GRDC). The GRDC is an international organization based in Germany, a branch of the World Meteorological Organization (WMO) that was established in 1988 to support scientific studies on global climate change and water resources management (GRDC, 2018) and (2) monthly precipitation datasets acquired from the Global Precipitation Climatology Project (GPCP) (Becker et al., 2013). The GRDC is an international organization based in Germany, a branch of the World Meteorological Organization (WMO) that was established in 1988 to support scientific studies on global climate change and water resources management (GRDC, 2018). Figure 3 shows ungauged areas and gauged catchments of Africa under consideration of a complete set of 12 months in a year (from January to December) during the period of 117 years (1901—2017). The shapefile of 25 major African basins was provided by the Food and Agriculture Organization of the United Nations (FAO) (FAO, 2009).

Formatted: Font: Times New Roman

Formatted: Line spacing: 1.5 lines

Formatted: Font: Times New Roman

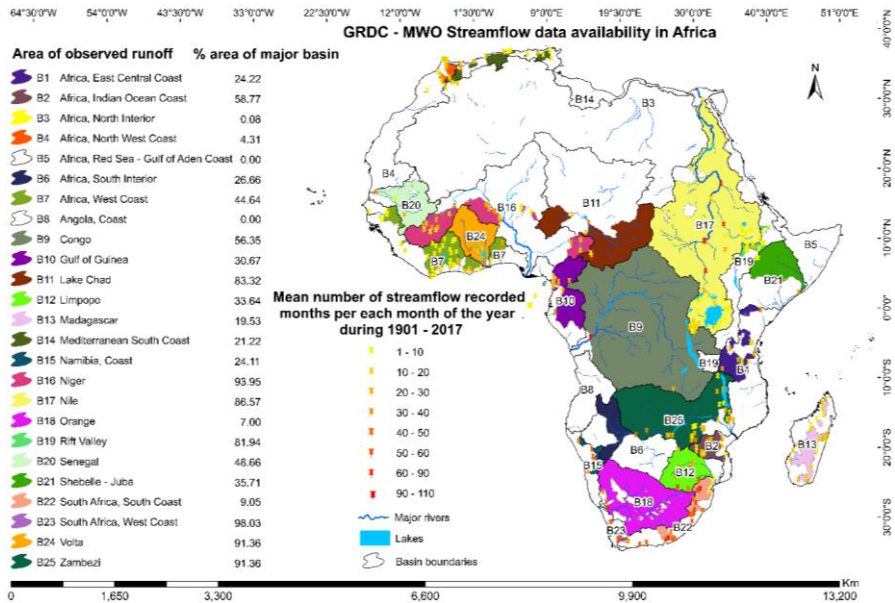


**Figure 3.** Land-area coverage of observed GRDC-WMO streamflow records within 25 major basins of Africa.

, and (2) monthly precipitation datasets acquired from the Global Precipitation Climatology Centre (GPCC) Full Data Gridded Monthly Totals Version 2018 (V.8) at 0.5° resolution for the period 1901–2016. GPCC product is a Rain-Gauges built on  
5 GTS-based and Historical Data that is operated by the German Weather Service (DWD) under the auspices of the World Meteorological Organization (WMO) (Markus et al., 2018).

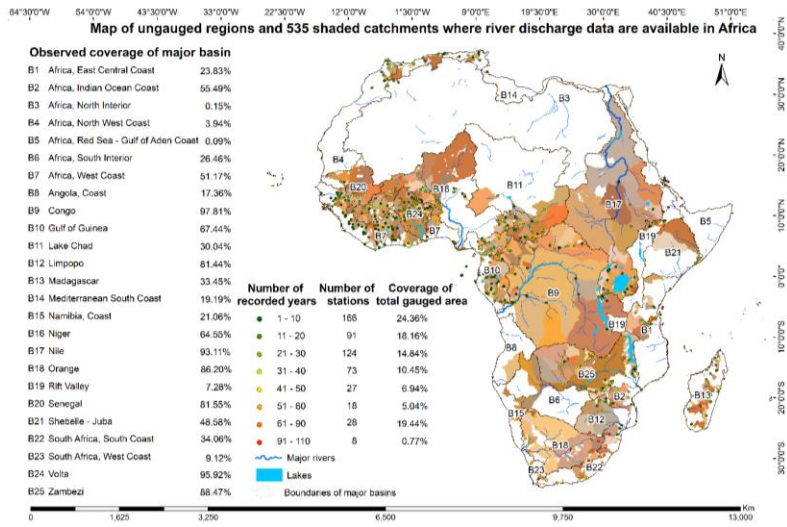


**Figure 3.** Distribution of 535 GRDC gauged catchments (covering  $\approx 47.43\%$  of the total African continent) and streamflow gauging stations (GRDC, 2018) within 25 major basins of Africa (FAO, 2009).

On account of discharge data that were discontinuously recorded in different months and various stations, and which could not allow the possibility of monthly or annual accurate trend analysis, the final results of the present study was carried out using were generated at the long-term monthly and annual mean monthly runoff and their corresponding rainfall input for the period 1901–2017. This method enabled us to obtain the streamflow records for all 12 months of the year and maximize the number of monitored basins, covering a total surface area of 12.37 million  $\text{km}^2$  ( $\approx 41.4\%$  of the total African continent). Given that, streamflow records were provided in cubic meter per second ( $\text{m}^3 \cdot \text{S}^{-1}$ ), monthly runoff depths at basin scale were calculated by Eq. (1):

$$R = \frac{(Q - 1000 - 24 - n - 3600)}{A} \quad (1)$$

where, R is an average runoff depth ( $\text{mm} \cdot \text{month}^{-1}$ ) for the drainage area or basin of interest A; A is a drainage area (basin) in  $\text{m}^2$ ; Q is river discharge ( $\text{m}^3 \cdot \text{S}^{-1}$ ) drained from the basin of interest A ( $\text{m}^2$ ); n is the number of days in each month. The long-term mean precipitation was computed from the Global Precipitation Climatology Centre (GPCC) version 7.0 at  $0.5^\circ$  resolution (Becker et al., 2013). This is the centennial GPCC Full Data Reanalysis of monthly global land-surface precipitation with a duration record of 10 years or longer from 75,000 stations worldwide. The temporal coverage of the dataset ranges from January 1901 to December 2013. The GPCC Full Data Reanalysis is the most accurate in-situ precipitation dataset which

Formatted: Font: Times New Roman

supports studies on regional climate monitoring, model validation, and water resources assessment (Becker et al., 2013). The remaining period starting from 2014 to 2017 was completed by monthly total precipitation calculated and resampled at 0.5° from the GPCC First-Guess Product at 1° resolution of daily global land surface precipitation based on the station database (SYNOP) available via the Global Telecommunication System (GTS) of the World Meteorological Organization (WMO) at the time of analysis (3–5 days after the end of the analysis month). This product contains the daily totals for a month on a regular latitude/longitude grid with a spatial resolution of 1° x 1° latitude by longitude (Schamm et al., 2014).

By following Eq. (2) (Kadioglu and ŞEN, 2001), we estimated the long-term monthly runoff coefficient is estimated as the ratio of long-term mean runoff depth to long-term rainfall intensity for each catchment. The monthly runoff coefficients were estimated for each month whenever runoff discharge was recorded. Then, all historical monthly precipitation for the study period 1901–2017 coefficients were summed and divided by the number of recorded months to obtain the long-term monthly average runoff coefficient for each station.

$$R_e = \frac{R}{P} \quad (2)$$

The annual runoff depth (mm·yr<sup>-1</sup>) is the total of monthly runoff depths for all 12 months of a year. The average annual runoff coefficient is estimated as the ratio of annual runoff depth (mm·yr<sup>-1</sup>) to the annual precipitation intensity (mm·yr<sup>-1</sup>).

$$Orc_b = \frac{Or_b}{P} \quad (1)$$

where,  $R_e$  is a  $Orc_b$  is the basin's observed average monthly runoff coefficient (dimensionless);  $R$ ,  $Or_b$  is the basin's observed runoff depth (mm·month<sup>-1</sup>) and  $P$  is precipitation intensity (mm·month<sup>-1</sup>).

The runoff coefficient is usually a suitable proxy to assess the correlation between precipitation and runoff due to its absolute capability to indicate the ratio of runoff (R) generated by the total precipitation (P) amount within a catchment (Kadioglu and ŞEN, 2001), it has values varying from 0 (low P-R correlation) to 1 (high P-R correlation) (Blume et al., 2007). In addition, runoff coefficient is very useful for rainfall runoff management in different land cover types since it can easily identify the ratio of rainwater flowed from each land use type under heterogeneous climate and physical conditions among different grids of the catchment. It may help to locate areas with high potential runoff risk which require special practices of stormwater management (Chen et al., 2007). Higher runoff coefficient values are often observed on impervious surfaces and unwell-managed croplands due to their low infiltration capacity compared to other land use classes such for example grasslands and forests (Goudie, 2000; Weng, 2001). Areas with low runoff coefficients are those with a relatively higher infiltration and/or evapotranspiration ( $E_T$ ) rates. Underground water storage change also plays significant role in runoff generation process throughout the alteration of soil moisture condition. However, in the long-term annual mean basis of water balance analysis, the estimation of terrestrial water storage change provides approximately zero values due to a variety of wet and dry seasons (Long et al., 2014).

Formatted: Font: Times New Roman

Formatted: Font: Times New Roman

Formatted: Indent: First line: 0"

Formatted: Font: Times New Roman

Formatted: Font: Times New Roman, English (United States)

Formatted: Font: Times New Roman, English (United States)

Formatted: Font: Times New Roman, English (United States)

Formatted: Font: Times New Roman

Formatted: Font: Times New Roman, Italic

Formatted: Font: Times New Roman

Formatted: Font: Times New Roman

### 2.2.2 Runoff coefficient estimation in ungauged basins catchments

Numerous studies have established different climatic geospatial datasets such as precipitation and surface temperature, etc., using interpolation algorithms based on a certain number of recorded locations directed by the other auxiliary variables (i.e.: DEM) to improve the results. Runoff coefficients over ungauged regions were estimated using the inter-gauged and ungauged parameter transfer method based on the hydrologic similarity feature zones established by means of overlay (intersect) technique applied to major runoff controlling factors, including AMC, CN, TWSC, T, TWI and slope that were selected among others based on their potential effect in runoff generation process as previously revealed by different researchers (Ahmed et al., 2014; Huang and Hu, 2009; Sanabria et al., 2013)(Liu and De Smedt, 2004; Bárdossy, 2007; Yuting et al., 2011; McCabe and Wolock, 2011). In this sense, the present study developed a hybrid interpolation method to estimate the  $R_c$  in ungauged basins of Africa using the Inverse Distance Weighting (IDW) interpolation algorithm directed by major runoff controlling factors (Potential runoff coefficient, surface temperature and precipitation). The potential runoff coefficient was estimated using the WetSpa (Water and Energy Transfer between Soil, Plants and Atmosphere) extension model (Liu and De Smedt, 2004) which incorporates three types of data inputs including land use and land cover, slope and soil texture classes as synthesized by a Table 1 (Liu and De Smedt, 2004). The soil texture and slope rasters were resampled to the same spatial resolution (300 m) of LULC maps and initial resolution of potential runoff coefficient, which is also resampled at 0.5° resolution (the original resolution of the temperature and precipitation datasets) using the zonal statistic method. The potential runoff coefficient for impervious surfaces (IMP) was estimated using Eq. (3) (Liu and De Smedt, 2004).

$$C_u = IMP + (1 - IMP) C_{grass} \quad (3)$$

where,  $C_u$  is the potential runoff coefficient for built up areas,  $C_{grass}$  is the potential runoff coefficient for grassland, and IMP is 0.50 that presents the percentage of impervious surfaces recommended for built up zones.

The LULC maps (Figure 4) used in this study were reclassified from time series of annual global Climate Change Initiative Land Cover (CCI LC) maps at 300 m spatial resolution covering a period of 24 years (1992—2015) (ESA CCI, 2017).

Formatted: Font: Times New Roman, English (United States)

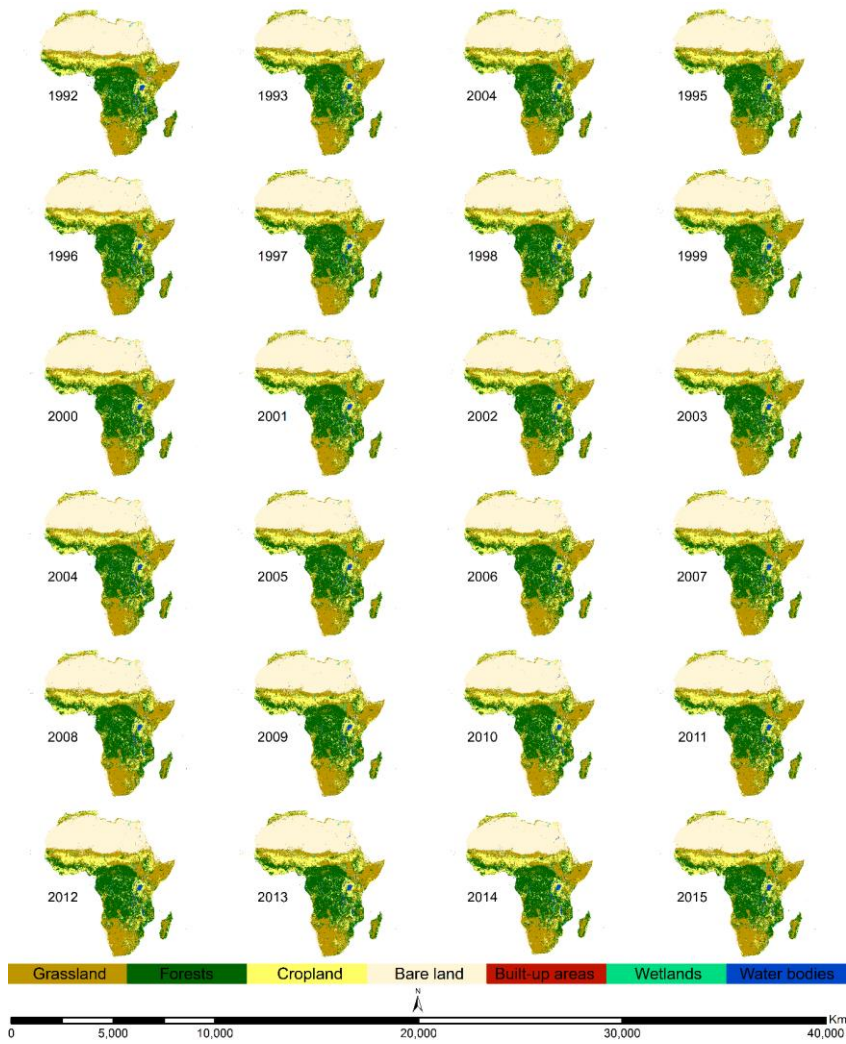


**Figure 4.** A time series of annual land cover maps of Africa with 7 classes (1992 – 2015).

. Inter-gauged and ungauged parameter transfer method is one of acceptable approach for parameter predictions in ungauged Basins (PUB) recommended in different hydrological studies (Bárdossy, 2007;Blöschl, 2006;Chiew et al., 2018). Several hydrologic models are available and utilized in different projects; but, most of them limited either due to their different input parameter requirements, a lot of time required for preparing input data, and complexity model setting (Lim et al., 2006).

5 Ungauged regions accounting 52.57% of the total continent of Africa seems to be larger extent compared to the recorded catchments (47.43% of African continent) (Figure 3) due to 31% of the continent occupied by the desert of Sahara (Cook and Vizy, 2015) where the runoff depths and runoff coefficient is approximately 0 due to absence of precipitation in this region. The remaining ungauged regions account only 21.57% of the total African continent and are distributed in different climatic zones where it is possible to predict their hydrologic conditions based on the observed parameters of neighbouring gauged

10 catchments. Using any other model for P-R correlation assessment it might be a double task since it would be necessary to calibrate the results using almost the same method of hydrologic similarity analysis.

#### **2.2.2.1 Estimation of direct runoff using the NRCS-CN method**

NRCS-CN is one of the ancient popular and efficient empirical hydrologic approaches adopted by various researchers worldwide for water resources planning and assessment, especially estimating the direct rainfall-runoff. It was developed in

15 1956 by the United States Department of Agriculture (USDA) Natural Resources Conservation Service (NRCS) (Cronshey, 1986;Silveira et al., 2000). This method is easily understandable, simple and useful for direct runoff prediction over ungauged catchments (Mishra et al., 2006). CN is generally considered as a major input parameter in many hydrologic models such as for example the Long-Term Hydrologic Impact Assessment (L-THIA) model (Lim et al., 2006), the Hydrologic Modelling System (HEC-HMS) (Engineers, 2008;Halwatura and Najim, 2013), The Chemicals, Runoff, and Erosion from Agricultural

20 Management Systems (CREAMS) (Knisel and Douglas-Mankin, 2012), Simulation of Production and Utilization of Rangelands (SPUR) model (Wright and Skiles, 1987). NRCS-CN method predicts the  $D_r_c$  and  $D_r$  by involving the land use and land cover (LULC) data, soil hydrological characteristics and antecedent soil moisture condition, according to an antecedent precipitation index (API) and precipitation (Cronshey, 1986). The LULC maps (Figure 4) used in this study were reclassified from time series of annual global Climate Change Initiative Land Cover (CCI-LC) maps at 300 m spatial resolution

25 covering a period of 24 years (1992 – 2015) (ESA-CCI, 2017).

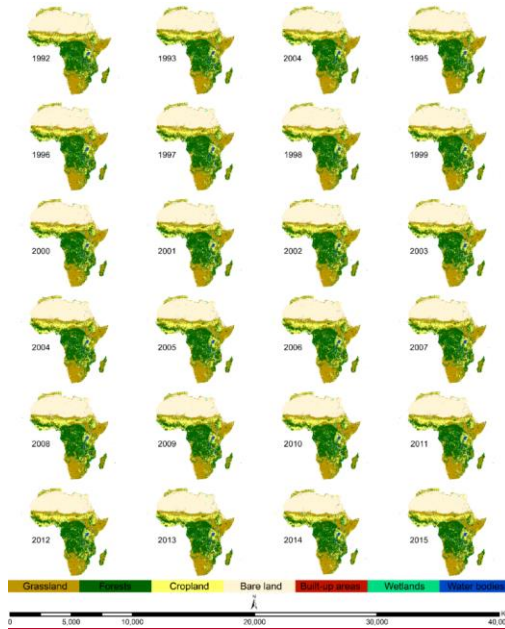


**Figure 4.** A time series of annual land cover maps (ESA-CCI, 2017) of Africa with reclassified 7 classes (1992 – 2015).

These land cover maps were originally classified from the landcover imagery captured by five different satellites, including the Advanced Very High-Resolution Radiometer (AVHRR), Medium Resolution Imaging Spectrometer Full Resolution and Reduced Resolution (MERIS FR and RR), SPOT-Vegetation (SPOT-VGT), Project for On-Board Autonomy, with the V standing for Vegetation (PROBA-V), Environmental Satellite-Advanced Synthetic Aperture Radar (ENVISAT-ASAR). The CCI-LC map 2015 was validated using the GlobCover map 2009 with two overall accuracy levels of 71.45% and 75.4% (ESA-CCI, 2017). Based on the CCI-LC product manual version 2.0 (ESA-CCI, 2017), we have reclassified all 24 CCI-LC maps were reclassified from the LCCS (Land Cover Classification System) legend to IPCC (Intergovernmental Panel on Climate Change) legend (Penman et al., 2003) that is consistent with a Table 1 of the Wetspa's potential runoff coefficient (Liu and De Smedt, 2004) are more compatible with the NRCS-CN structure.

**Table 1.** Potential runoff coefficient for different land use and land cover types, slope and soil texture classes (Liu and De Smedt, 2004). Sa: Sand, LoSa: Loamy sand, SaLo: Sandy loam, Lo: Loam, SiLo: Silty loam, Si: Silt, SaCilo: Sandy clay loam, Cilo: Clay loam, SiCilo: Silty clay loam, SaCl: Sandy clay, SiCl: Silty clay, Cl: Clay.

Formatted: Font: Times New Roman





have gaps over the Sahara desert, in this region the soil texture was classified from the WorldGrids' s sand, clay, and silt fractions available at 1 km spatial resolution (Hengl et al., 2014). The slope map at 300-m resolution (Figure 5) was established from the Global Multi-resolution Terrain Elevation Data 2010 (GMTED2010) available at 250-m spatial resolution of the U.S. Geological Survey (USGS) and the National Geospatial-Intelligence Agency (NGA) (Danielson and Gesch, 2011).

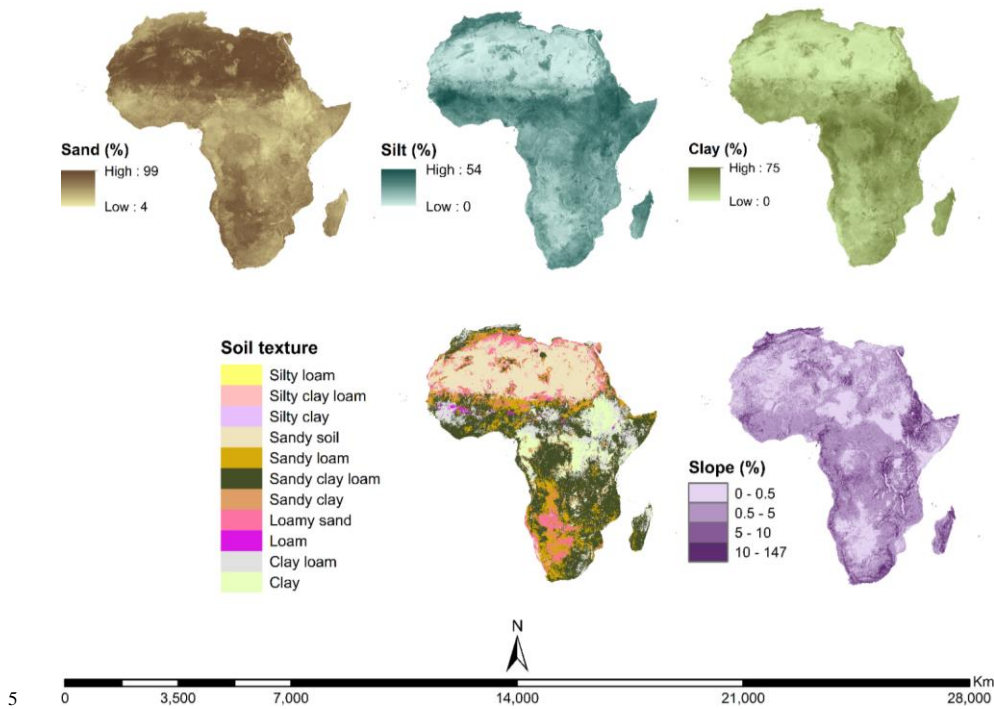


**Table 2.** LULC classes and their corresponding HSG, soil texture and CN (adapted from (Yeo et al., 2004;Cronshey, 1986;Sumarauw and Ohgushi, 2012).

<u>LULC</u>	<u>Soil Texture</u>	<u>HSG</u>	<u>CN</u>
Grass	Sand, loamy sand, or sandy loam	A	35

	<u>Silt loam or loam</u>	<u>B</u>	<u>56</u>
	<u>Sandy clay loam</u>	<u>C</u>	<u>70</u>
-	<u>Clay loam, silty clay loam, sandy clay, silty clay, or clay</u>	<u>D</u>	<u>77</u>
<u>Forrest</u>	<u>Sand, loamy sand, or sandy loam</u>	<u>A</u>	<u>30</u>
	<u>Silt loam or loam</u>	<u>B</u>	<u>55</u>
	<u>Sandy clay loam</u>	<u>C</u>	<u>70</u>
-	<u>Clay loam, silty clay loam, sandy clay, silty clay, or clay</u>	<u>D</u>	<u>77</u>
<u>Agriculture</u>	<u>Sand, loamy sand, or sandy loam</u>	<u>A</u>	<u>64</u>
	<u>Silt loam or loam</u>	<u>B</u>	<u>75</u>
	<u>Sandy clay loam</u>	<u>C</u>	<u>82</u>
-	<u>Clay loam, silty clay loam, sandy clay, silty clay, or clay</u>	<u>D</u>	<u>85</u>
<u>Barren</u>	<u>Sand, loamy sand, or sandy loam</u>	<u>A</u>	<u>77</u>
	<u>Silt loam or loam</u>	<u>B</u>	<u>86</u>
	<u>Sandy clay loam</u>	<u>C</u>	<u>91</u>
-	<u>Clay loam, silty clay loam, sandy clay, silty clay, or clay</u>	<u>D</u>	<u>94</u>
<u>Urban</u>	<u>Sand, loamy sand, or sandy loam</u>	<u>A</u>	<u>81</u>
	<u>Silt loam or loam</u>	<u>B</u>	<u>88</u>
	<u>Sandy clay loam</u>	<u>C</u>	<u>91</u>
-	<u>Clay loam, silty clay loam, sandy clay, silty clay, or clay</u>	<u>D</u>	<u>93</u>
<u>Wetland</u>	<u>Sand, loamy sand, or sandy loam</u>	<u>A</u>	<u>0</u>
	<u>Silt loam or loam</u>	<u>B</u>	<u>62</u>
	<u>Sandy clay loam</u>	<u>C</u>	<u>74</u>
-	<u>Clay loam, silty clay loam, sandy clay, silty clay, or clay</u>	<u>D</u>	<u>85</u>
<u>Water</u>	<u>Sand, loamy sand, or sandy loam</u>	<u>A</u>	<u>100</u>
	<u>Silt loam or loam</u>	<u>B</u>	<u>100</u>
	<u>Sandy clay loam</u>	<u>C</u>	<u>100</u>
-	<u>Clay loam, silty clay loam, sandy clay, silty clay, or clay</u>	<u>D</u>	<u>100</u>

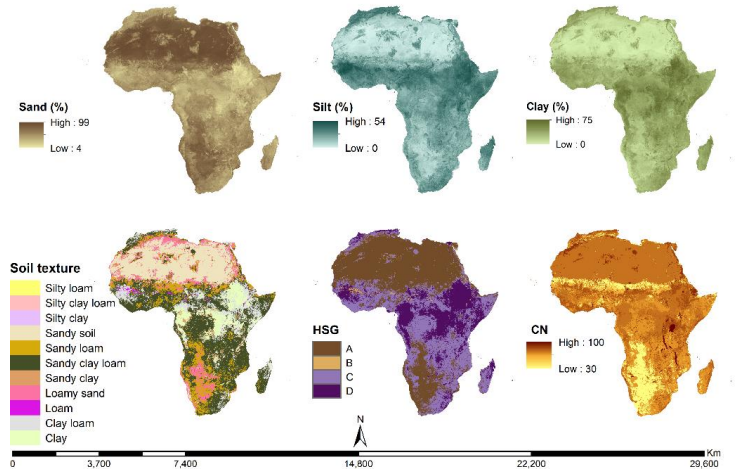


**Figure 5.** Maps of sand, clay, and silt fractions, soil texture and slope of Africa, hydrological soil group (HSG) and long-term mean curve number (CN) unadjusted by AMC (1992 – 2015).

The long-term monthly land surface temperature (Figure 6) Adjusted long-term monthly CN maps (Figure 6) were obtained employing antecedent soil moisture condition (AMC) (Figure 6) using equations (2) and (3) (Hong et al., 2007; Zeng et al., 2017).

$$CN_i^I = \frac{CN_i^{II}}{2.281 - 0.01281 * CN_i^{II}} \quad (2)$$

$$CN_i^{III} = \frac{CN_i^{II}}{0.427 - 0.00573 * CN_i^{II}} \quad (3)$$

$C^I$ ,  $C^{II}$ , and  $C^{III}$  are corresponding to AMC I (dry), AMC II (normal), and AMC III (wet), respectively, determined utilizing total 5-day antecedent precipitation index (API) and season types (dormant or passive and active or growing seasons) (Table 3) (Silveira et al., 2000; Hong et al., 2007). The growing season is considered as the active (wet) season with the precipitation intensity  $> 100 \text{ mm} \cdot \text{month}^{-1}$ , whilst, the passive (dry) season has a precipitation intensity  $< 100 \text{ mm} \cdot \text{month}^{-1}$  (Murray-Tortarolo et al., 2017).

**Table 3.** Seasonal rainfall limits for AMC (Silveira et al., 2000; Hong et al., 2007; Mishra and Singh, 2006).

AMC group	Total 5-day API (mm)	
	Dormant (passive) season	Growing (active) season
I	$< 13$	$< 36$
II	$13 - 28$	$36 - 53$
III	$\geq 28$	$\geq 53$

Formatted: Font: 9 pt, Bold

Formatted: Font: Times New Roman, 9 pt

Formatted: Normal, Left, Space After: 10 pt

Formatted: Font: 9 pt

Formatted: Font: Times New Roman, 9 pt

Five-day API was estimated using the GPCC Full Data Daily Product V.2018 of daily global land-surface precipitation totals. This product is available at a regular latitude/longitude grid with a spatial resolution of 1° and covers the time period from January 1982 to December 2016 (Anja et al., 2018). The API was estimated following Eq. (4) (Kohler and Linsley, 1951; Heggen, 2001).

$$API = \sum_{t=1}^i P_t * k^{-t} \quad (4)$$

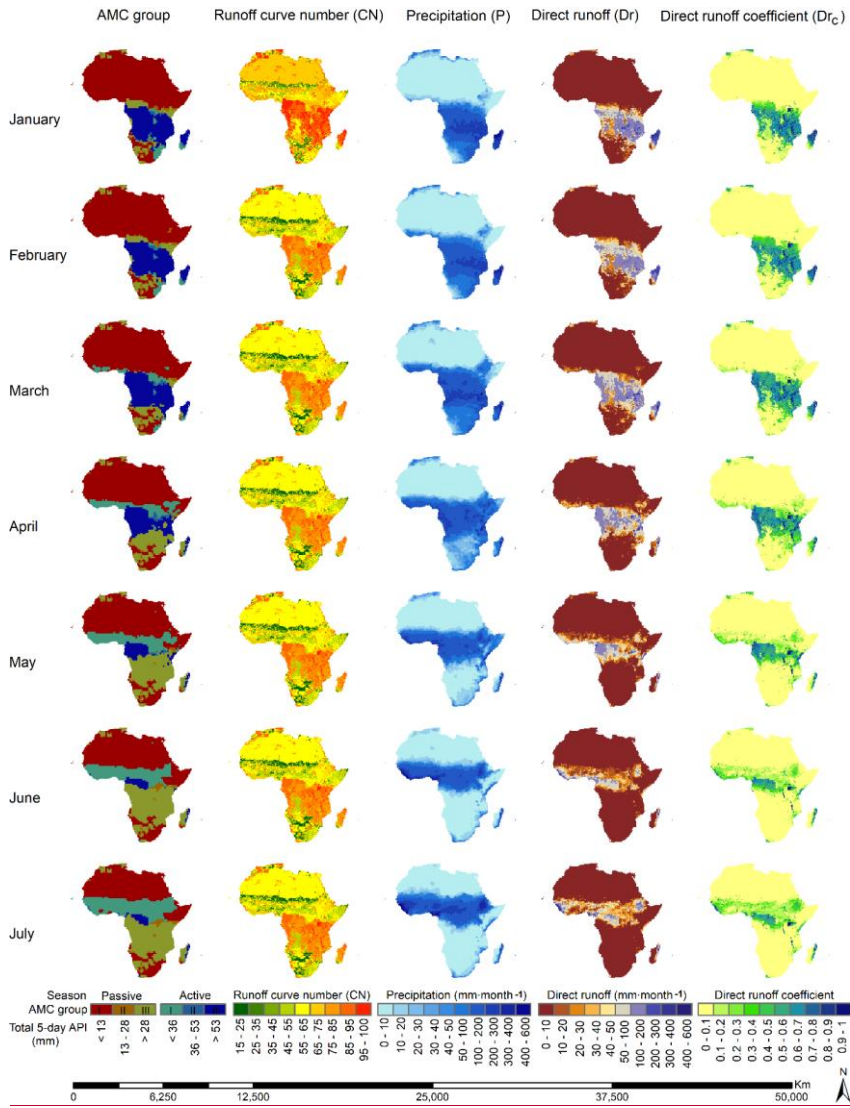
where,  $i$  is the number of antecedent days,  $P_t$  is the precipitation amount during day  $t$ , and  $k$  is a decay constant. It has been revealed that  $k$  factor is not critical, its values range from 0.85 to 0.90 over most of the eastern and central portions of the United States where it was well tested (Kohler and Linsley, 1951), and this study used a value of 0.90 that is recommended for the basins without a measured  $k$  decay constant (Abdi et al., 2017; Viessman Jr and Knapp, 1977; Heggen, 2001). The NRCS-CN method was modified by different researchers depending on the climatic condition of their study area. The most frequently modified parameter was the initial abstraction coefficient ( $\lambda$ ), arguing that the assumption of the  $\lambda = 0.2$  in the original SCS-CN method seems to be high and suggested that  $\lambda$  with values between 0.01 and 0.05 are more realistic and recommended a value of  $\lambda = 0.05$  (5% of the storage is assumed as the initial abstraction instead of 20%) because it involves either both lower CN values and small rainfall amount (Yuan et al., 2014; Beck et al., 2009; Shi et al., 2009; Hawkins, 1993; Ponce and Hawkins, 1996; Woodward et al., 2003; Lim et al., 2006). Based on these recent studies, our study used an adjusted SCS-CN equation with a value of  $\lambda = 0.05$  as demonstrated by Hawkins (1993) with the equations (5), (6) and (7).

$$Dr = \begin{cases} 0 & \text{for } P \leq 0.05 * S \\ \frac{(P - 0.05 * S_{0.05})^2}{P + 0.95 * S_{0.05}} & \text{for } P > 0.05 * S \end{cases} \quad (5)$$

$$S_{0.05} = 1.33 * S_{0.20}^{1.15} \quad (6)$$

$$S_{0.20} = \frac{2400}{CN} - 254 \quad (7)$$

where,  $Dr$  = the direct runoff (mm),  $P$  = rainfall (mm) (Figure 6),  $S$  is the maximum potential soil water retention (mm), and  $CN$  is the curve number (dimensionless).  $I_0 = 0.05 * S$  is the initial abstraction (all losses before runoff begins).  $Dr_c$  = the direct runoff coefficient (dimensionless) (Figure 6).  $S$  is related to the soil and land cover conditions of the watershed through the  $CN$  which has a range of 0 to 100 values.



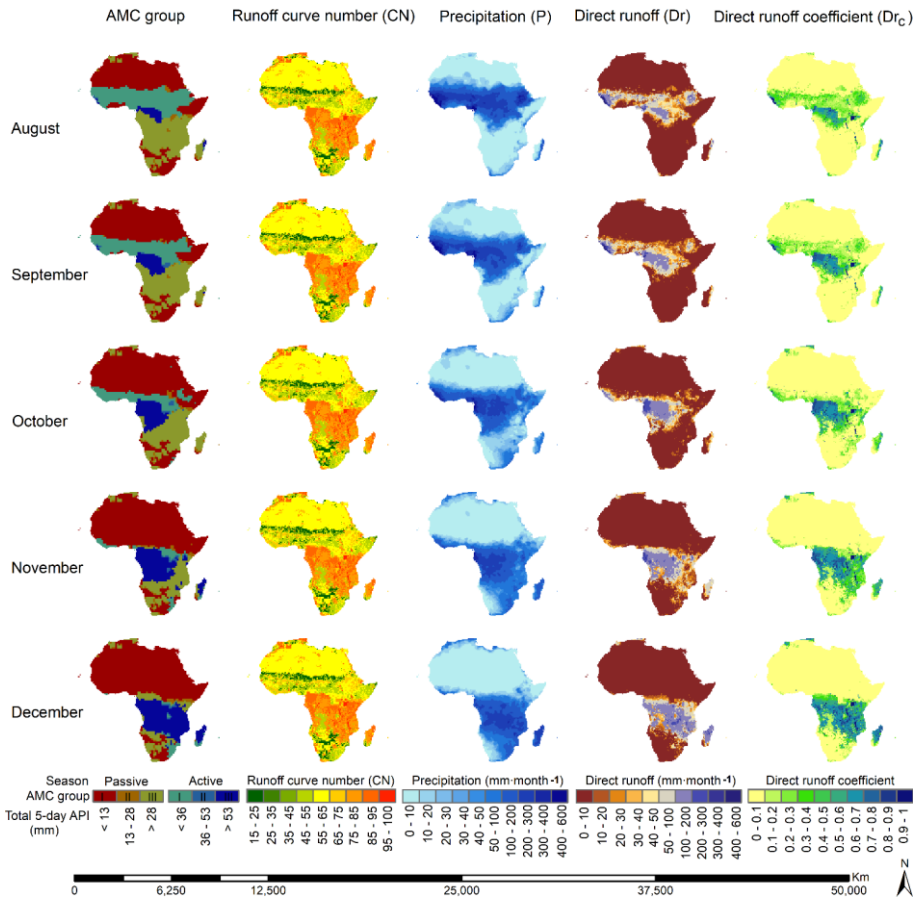


**Figure 6.** Maps of the runoff curve number (CN) adjusted according to antecedent soil moisture condition (AMC), precipitation (P), direct runoff depths (Dr) and direct runoff coefficients ( $Dr_c$ ).

### 2.2.2.2 Downscaling process of the runoff discharges

- 5 Equations (8), (9), (10), (11), (12), (13), and (14) express the process used to downscale the observed runoff coefficients and runoff depths from basin scaled to 0.5° grid spatial resolution (Figure 7) based on the direct runoff distributions within different grids of each gauged catchment. This approach provides google results since the mean of observed gridded runoff coefficients and runoff depths equals to the catchment's average observed runoff coefficients and runoff depths, respectively.

$$Drv_g = 0.001 * Dr_g * G \quad (8)$$

$$Drv_b = 0.001 * Dr_b * A \quad (9)$$

$$\phi = \frac{Drv_g * 100}{Drv_b} \quad (10)$$

$$Orv_b = 0.001 * Or_b * A \quad (11)$$

$$5 \quad Orv_g = \frac{Orv_b * \phi}{100} \quad (12)$$

$$Or_g = \frac{Orv_g}{G} * 1000 \quad (13)$$

$$Orc_g = \frac{Or_g}{P_g} \quad (14)$$

where, ( $\phi$ ) is the percent contribution of each grid's direct runoff volume ( $Drv_g$ ) in  $m^3 \cdot month^{-1}$  to its corresponding basin's direct runoff discharge ( $Drv_b$ ) in  $m^3 \cdot month^{-1}$ ,  $Dr_g$  is the grid's direct runoff depth ( $mm \cdot month^{-1}$ ),  $Dr_b$  is the basin's average direct runoff depth ( $mm \cdot month^{-1}$ ),  $G$  is the size of a grid in  $m^2$ , 0.001 and 1000 are the numbers for unities conversion,  $A$  is the drainage area of basin in  $m^2$ ,  $Orv_b$  is the basin's observed runoff discharge ( $m^3 \cdot month^{-1}$ ),  $Or_b$  is the basin's observed runoff depth ( $mm \cdot month^{-1}$ ),  $Or_g$  is the grid's observed runoff depth ( $mm \cdot month^{-1}$ ),  $Orc_g$  is the grid's observed runoff coefficient (dimensionless),  $P_g$  is the grid's precipitation intensity ( $mm \cdot month^{-1}$ ).

### 2.2.2.3 Application of inter-gauged and ungauged basin parameter transfer approach

15 Overlay (intersect) is one of useful geospatial overlay methods that stacks several different types of dataset with the same georeferencing system on top of each other in order to assess the relationship between features of each location. Overlay method has been used in different applications such as relationship analysis between rainfall distribution and elevation, examination of environmental sensitivity based on slope, surface drainage, soil erosion and other environmental parameters (Zhu, 2016). This method was applied to the present study in order to establish a unique zonal feature dataset that combines  
 20 together a set of important physical-climate variables which control the runoff (AMC, CN, TWSC, T, and TWI and slope). Each intersection of these variables falls within gauged and ungauged grids at the same time, here immediately ungauged grids receive an average of observed runoff coefficient locating within the same intersection. This operation was achieved using the "Zonal Statistics as Table Tool" available in the Spatial Analyst Tools of the ArcMap v.10.5" where, hydrologic similarity's zonal feature dataset were considered as "Input raster or feature zone data", and downscaled observed runoff as "Input value  
 25 raster".

The hydrological similarity analysis involved AMC (Figure 6) based on its potential capability to separate the drying and wetting areas, whilst CN (Figure 6) helps to recognize the effect of land use and soil characteristics in runoff generation process. According to the water balance budget, during the rainy seasons water soaks into pervious ground and once filled in

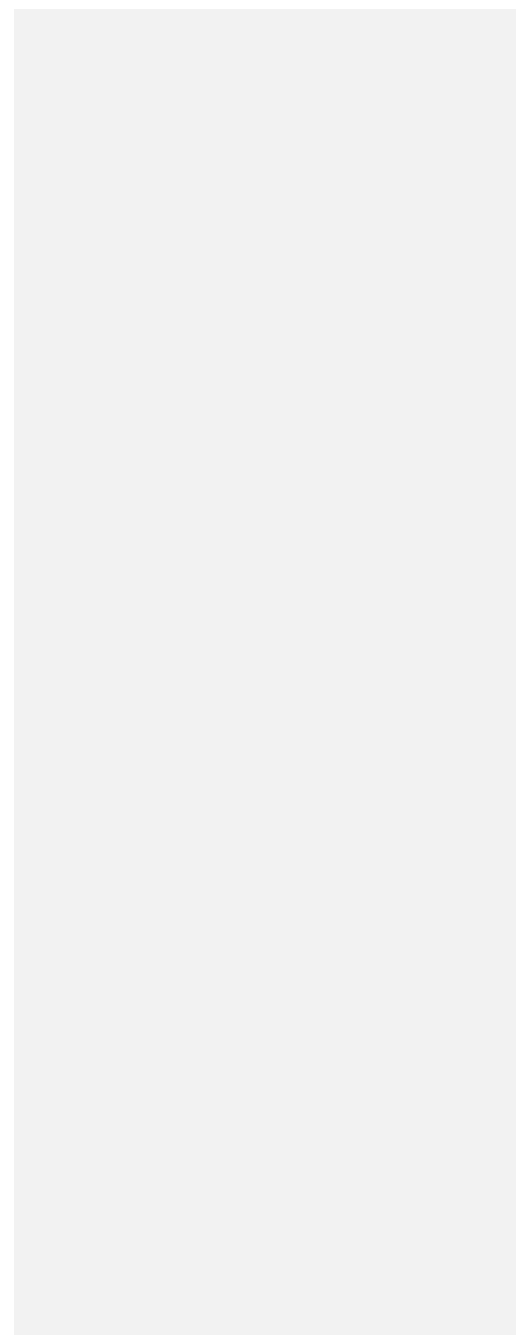
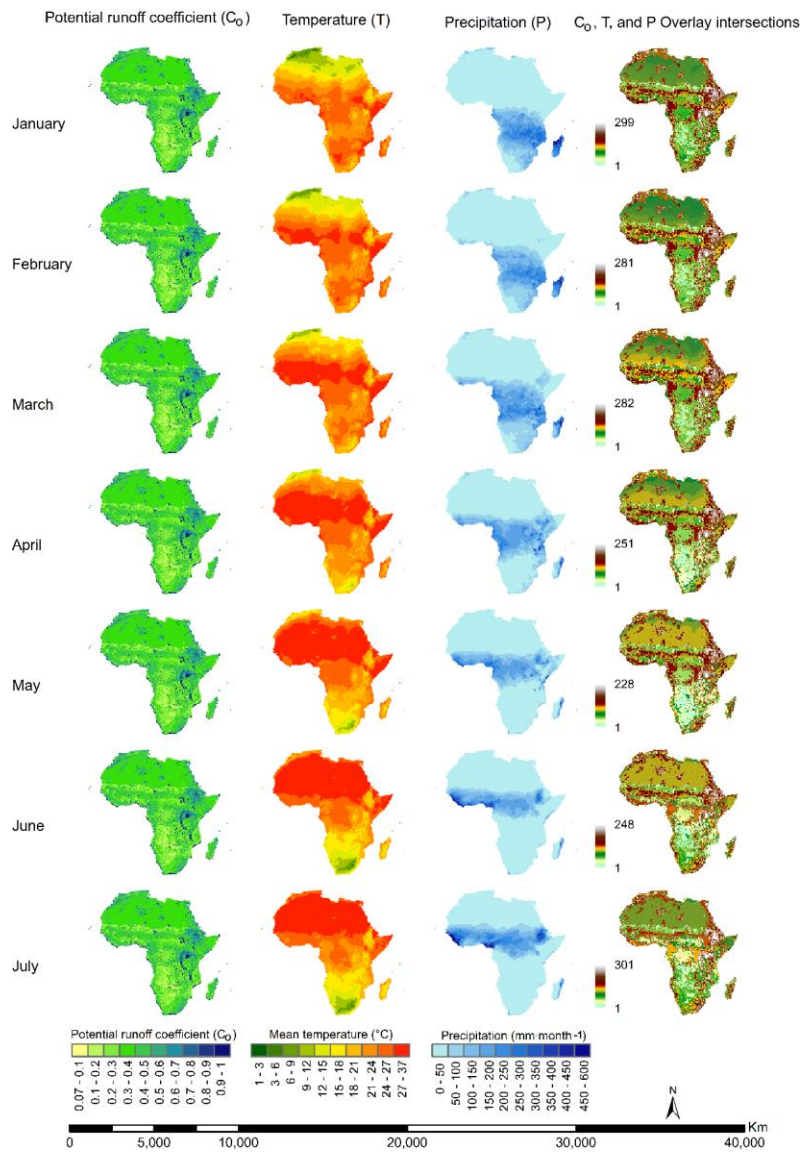
soil porosities starts to flow into rivers and lakes resulting in an increased level of underground water (aquifers) and surface water reservoirs (rivers, lakes and oceans); in impervious surface rainwater flow forward immediately into surface water reservoirs. Accumulation of water infiltrations improves soil moisture condition and boosts the rate of runoff depths while, a declining water storage phenomenon leads to lower amount of runoff discharge (Edwards et al., 2015). Apart from the natural cause of water storage change fluctuations (i.e.: rainfall and evapotranspiration), human activities (i.e.: water storage for hydropower generation and its release, irrigation, water consumption, etc.) also affect the change of water storage and as well river discharge volume. However, the change of water storage is generally controlled by climate and seasons patterns more than human factors (Edwards et al., 2015).

In order to incorporate the effect of water storage change in hydrologic similarity analysis, this study used the long-term monthly terrestrial water storage change (Figure 7) computed from the Center for Space Research (CSR) Gravity Recovery and Climate Experiment (GRACE) RL05 mascon solutions available at 1° resolution for the period starting from April 2002 to June 2016. The Gravity Recovery and Climate Experiment (GRACE) mission was launched in March 2002 under the NASA Earth System Science Pathfinder (ESSP) Program. GRACE is jointly implemented by the US National Aeronautics and Space Administration (NASA) and German Aerospace Center (DLR) (Save et al., 2016).

The land-surface temperature also plays a big role in water balance where, hot regions are often characterized by higher evapotranspiration rates compared to cold or temperate regions. The long-term monthly land-surface temperature (Figure 7) used in this study was calculated from the 4.01 release of the CRU TS (Climatic Research Unit Timeseries) dataset spanning a period of 116 years (1901 – 2016) (Harris et al., 2014). This dataset was developed, subsequently updated, improved and maintained with support from a number of funders, principally by the UK's Natural Environment Research Council (NERC) and the US Department of Energy. Long-term support is currently provided by the UK National Centre for Atmospheric Science (NCAS), a NERC collaborative center (Harris et al., 2014).

**Formatted:** Indent: First line: 0.25", Space After: 0 pt, Add space between paragraphs of the same style

**Formatted:** Font: Times New Roman



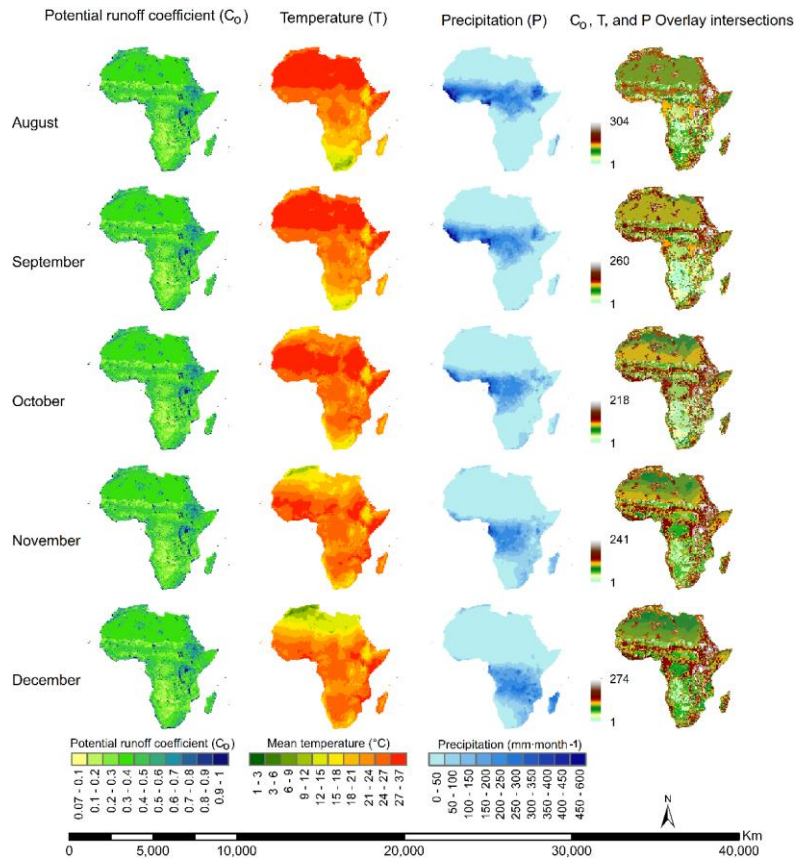


Figure 6. Maps for runoff controlling factors: potential runoff coefficient ( $C_0$ ), surface temperature (T) and precipitation (P) utilized to establish the  $C_0$ , T and P overlay intersections for the interpolation guidance of the observed runoff coefficient ( $R_o$ ).

### 2.2.3 Estimation of runoff and annual evapotranspiration

The long-term runoff depth was estimated using Eq. (4).

$$R = R_c \times P \quad (4)$$

where,  $R$  is a runoff depth ( $\text{mm}\cdot\text{month}^{-1}$ ),  $R_c$  is a runoff coefficient (dimensionless), and  $P$  is the precipitation intensity ( $\text{mm}\cdot\text{month}^{-1}$ ). The long-term annual  $R_c$  is the average of all monthly long-term  $R_c$  for the period starting from 1901 to 2017.

The current study estimated the long-term annual mean evapotranspiration according to the principle of water budget expressed by Eq. (5) referring to the concept water balance, where ground water changes is approximately zero on the long-term annual period basis due to the patterns of wet and dry seasons of the year (Edwards et al., 2015).

$$E_T = P - R \quad (5)$$

where,  $E_T$  is a long-term mean evapotranspiration in  $\text{mm}\cdot\text{yr}^{-1}$ ,  $P$  is a long-term mean precipitation in  $\text{mm}\cdot\text{yr}^{-1}$ , and  $R$  is a long-term mean runoff depth in  $\text{mm}\cdot\text{yr}^{-1}$ . Thus, the evapotranspiration coefficient ( $ET_c$ ) can be expressed as the ratio of evapotranspiration to precipitation intensity received within the same basin and the identical period (Yang et al., 2018) as presented by Eq. (6):

$$ET_c = \frac{E_T}{P} \quad (6)$$

The topography also acts on water flow movement and infiltration; where higher runoff depths are mostly found in regions with steep slopes more than areas with flat and gentle slopes (Ogden et al., 2011). Sometimes, digital elevation model (DEM) is used directly as a parameter that represents the impact of the surface shapes and feature on the hydrological process (Xiao et al., 2017). The dataset of topographic wetness index (TWI) that is also called the Compound Topographic Index (CTI) was developed by Beven and Kirkby (1979) within the runoff model TOPMODEL due to the effect of topography on soil moisture (BEVEN and Kirkby, 1979). TWI (Eq. 15, 16 and 17) that combines local upslope contributing area and slope is commonly used to quantify topographic control on hydrological processes. Higher TWI values represent drainage depressions which are often wet and associated with greater runoff depths compared to crests and ridges relatively with the lower TWI values and dry surfaces that suck a lot of water amount before the beginning of water flow process (Liu et al., 2015; Sørensen et al., 2006; Xiao et al., 2017). TWI and slope parameters (Figure 7) derived from the HydroSHEDS datasets at 15 arc-second resolution (Lehner et al., 2008) were incorporated in the hydrologic similarity analysis of this study in order to separate areas with different topographic features.

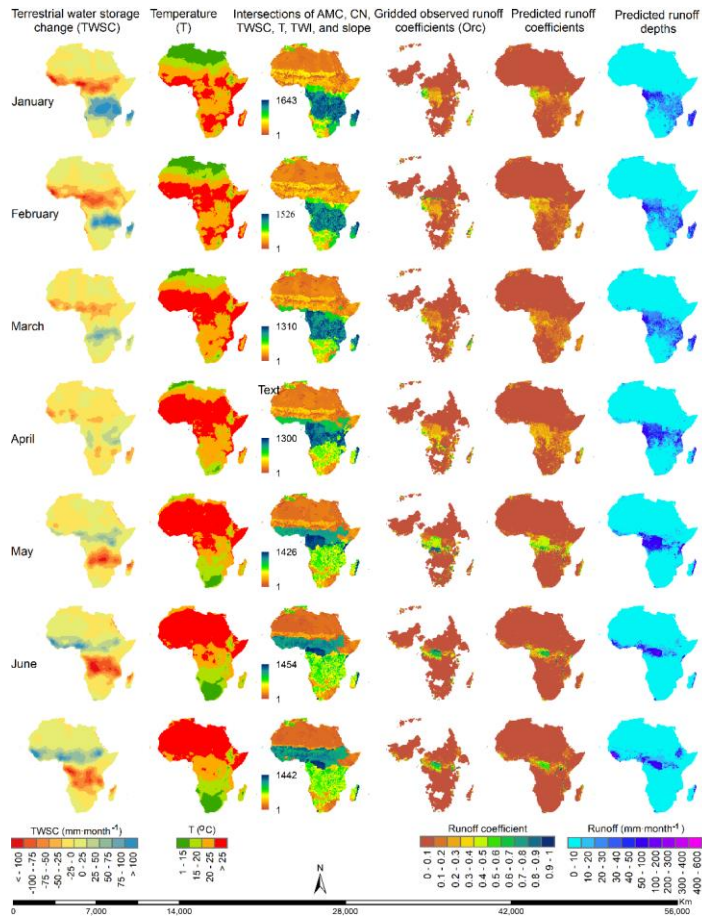
$$TWI = \ln \left( \frac{\alpha}{\tan \beta} \right) \quad (15)$$

$$\alpha = (f + 1) * G \quad (16)$$

$$\beta = (m * (\pi/2))/90$$

(17)

where,  $\alpha$  is the upslope area draining through a certain point per unit contour length and  $\beta$  is the slope in radians,  $f$  is the flow accumulation calculated from the flow direction that is generated in DEM (meter unity),  $G$  is the cell size in  $m^2$ ,  $m$  is the slope in degrees,  $\pi$  is pi equals to 3.141592.



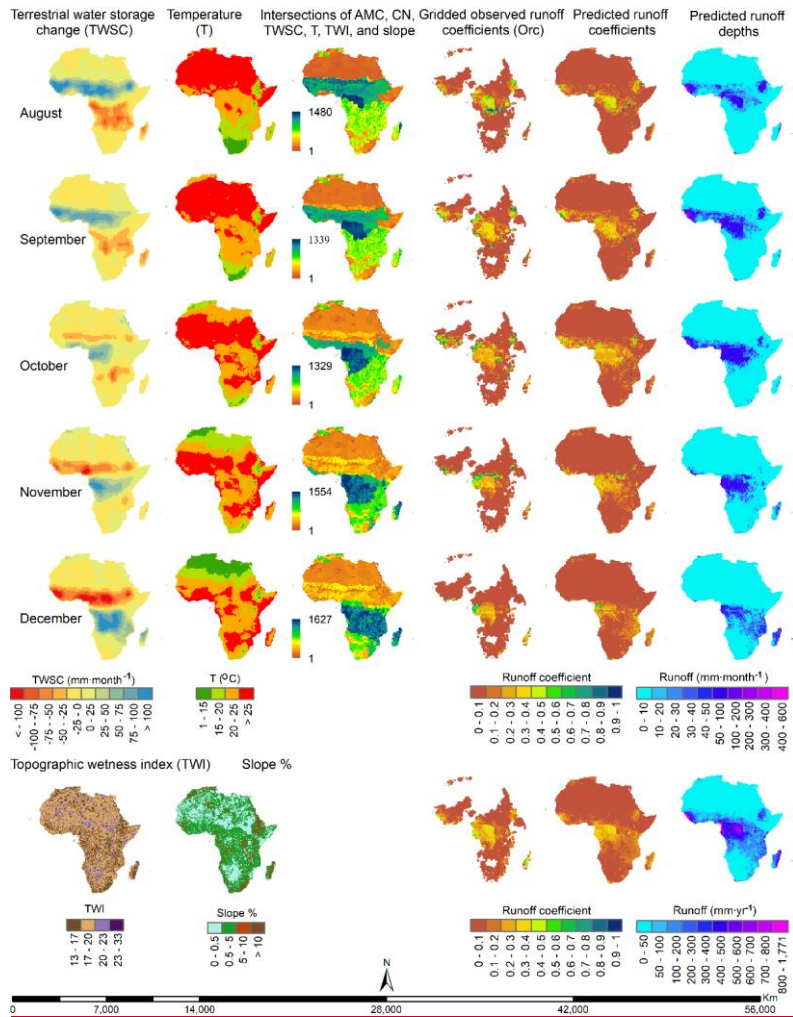


**Figure 7.** Estimated runoff coefficients and runoff depths based on gridded observed runoff coefficients transferred using inter-gauged and ungauged parameter transfer approach, according to hydrological similarity feature dataset resulted from an overlay (intersect) of the runoff controlling factors (AMC, CN (Figure 6), TWSC, T, TWI, and slope).

### 3 Results

Figure 78 presents the final resultant maps obtained by means of the methods above-described in sections 2.2.1 and 2.2.2. Gridded long-term mean monthly and annual mean runoff coefficient coefficients (RC), precipitation (P), and runoff depths (R) were developed at 0.5° spatial resolution for the period starting from (1901 to 2017/2016) and utilized to produce the generate zonal statistics at the continental level; (Figure 9 and 10), within 25 major basins and (Figure 11), 55 countries of Africa; (Figure 12) and as well latitudinal profile (Figure 14 and Table 4).

Formatted: Font: Times New Roman

Formatted: Space Before: 12 pt

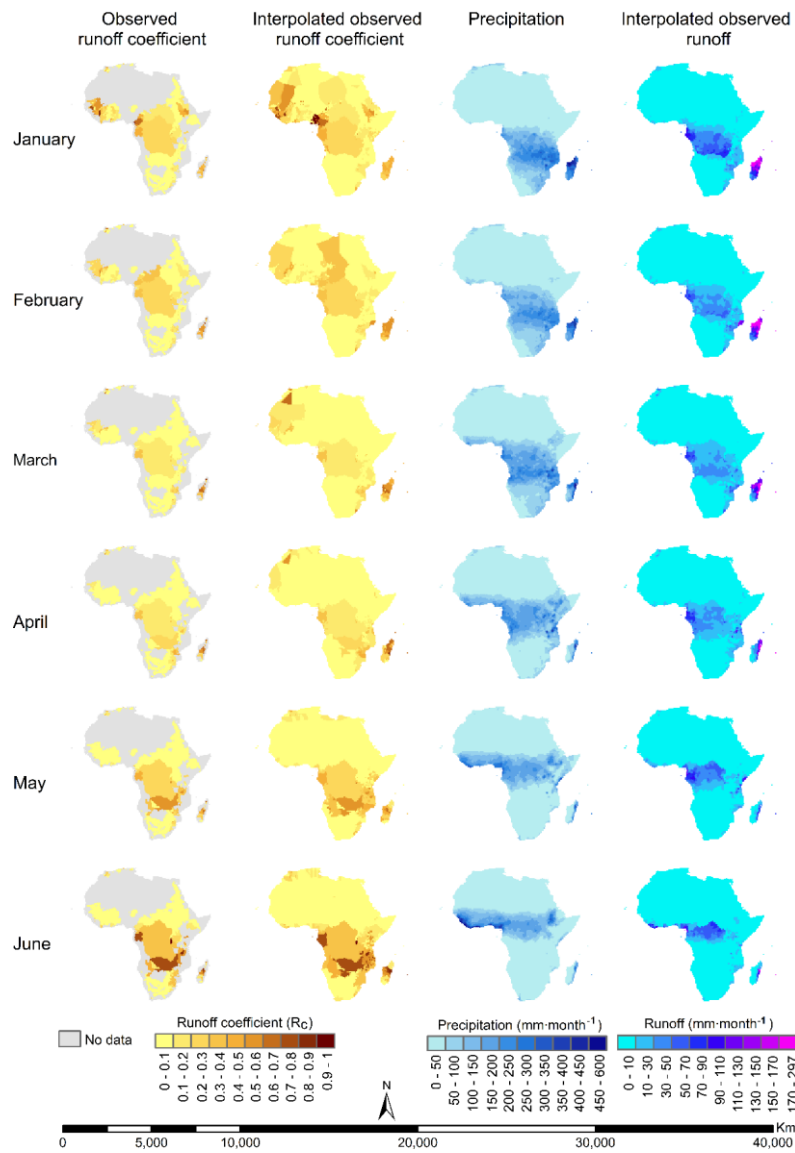
Formatted: Font: Times New Roman

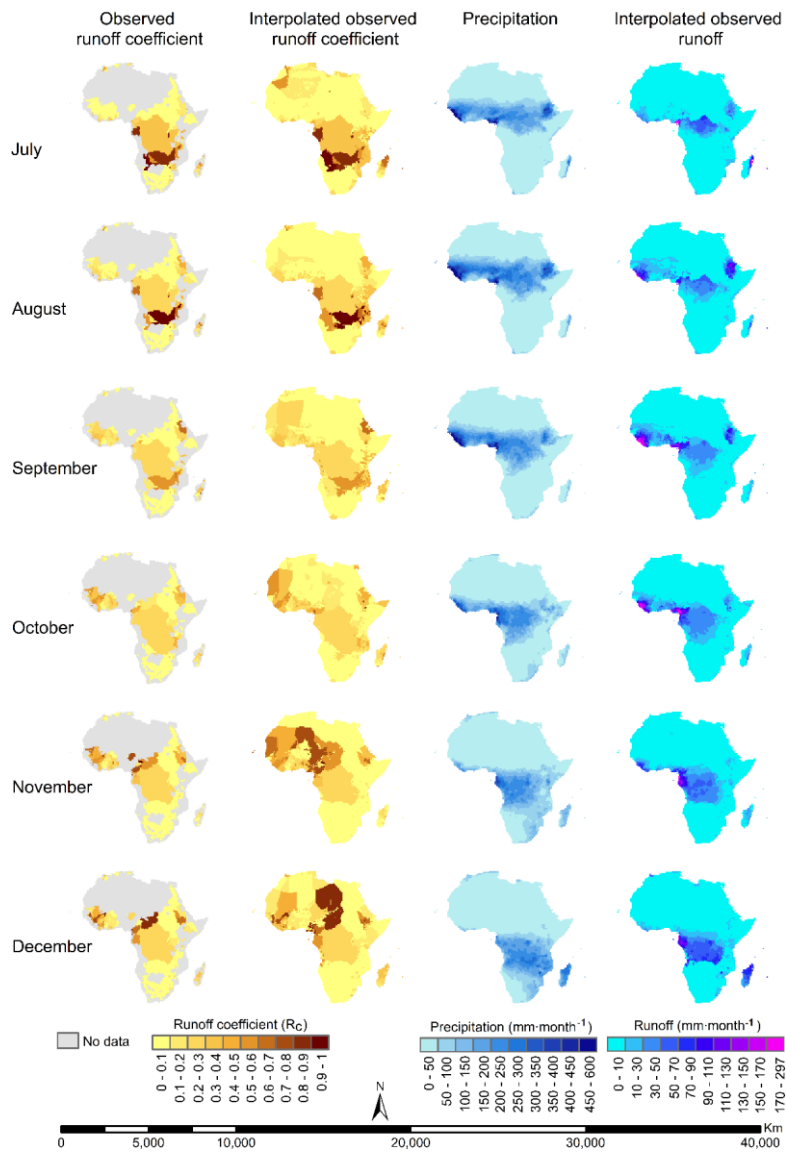
Formatted: Font: Times New Roman

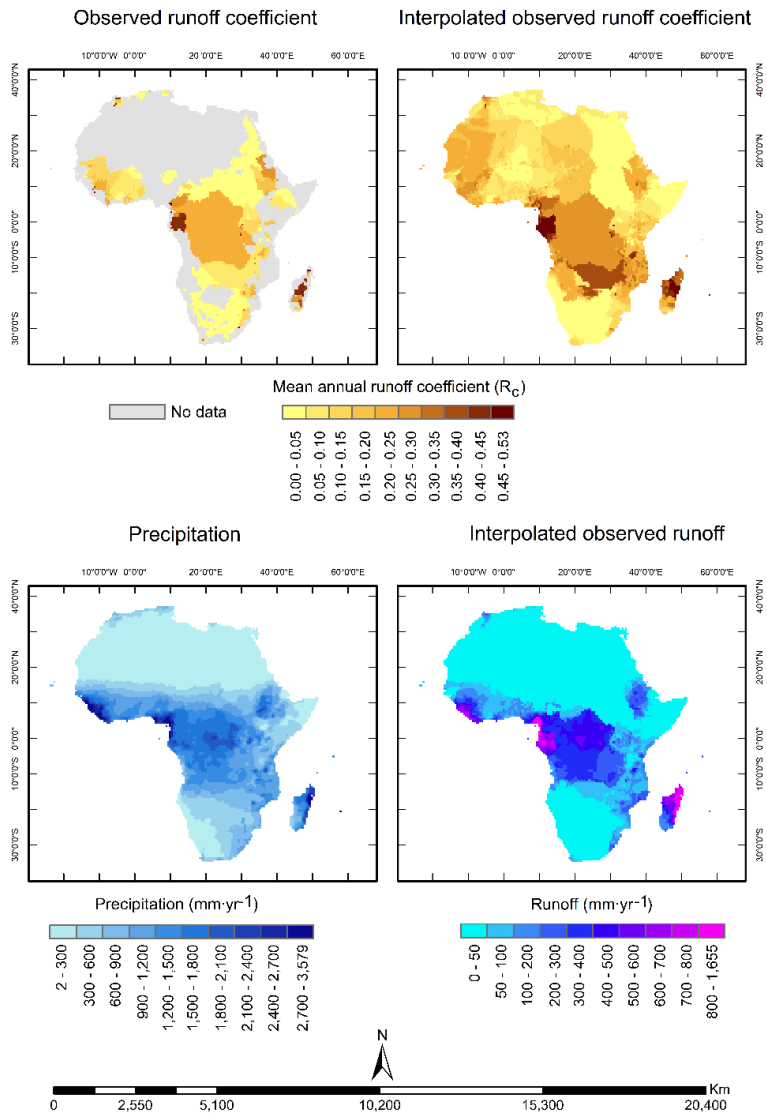
Formatted: Font: Times New Roman

Formatted: None, Space Before: 0 pt, Don't keep with next

Formatted: Font: Times New Roman







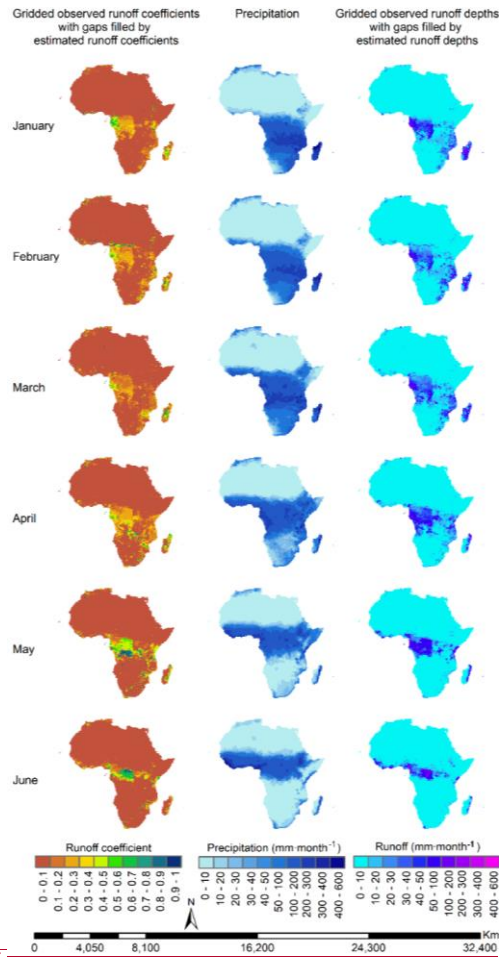
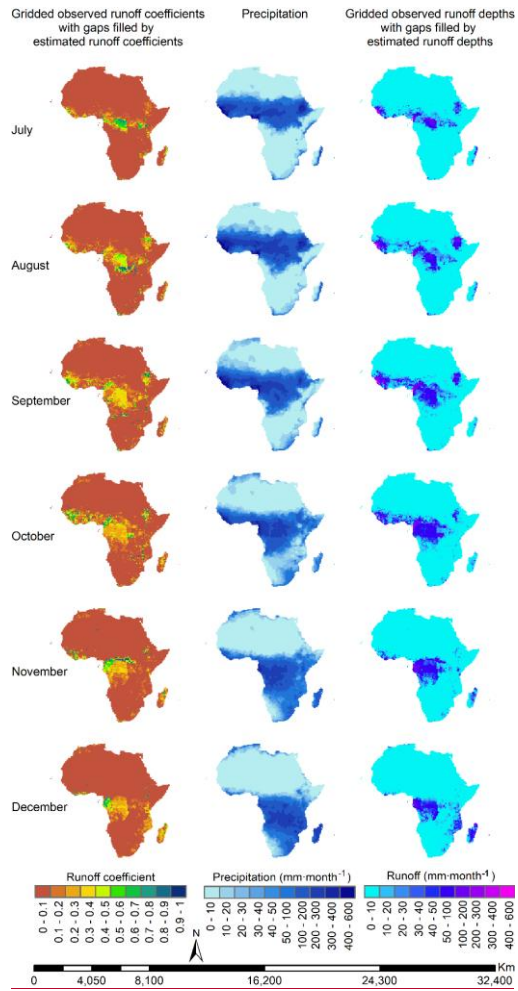


Figure 7.



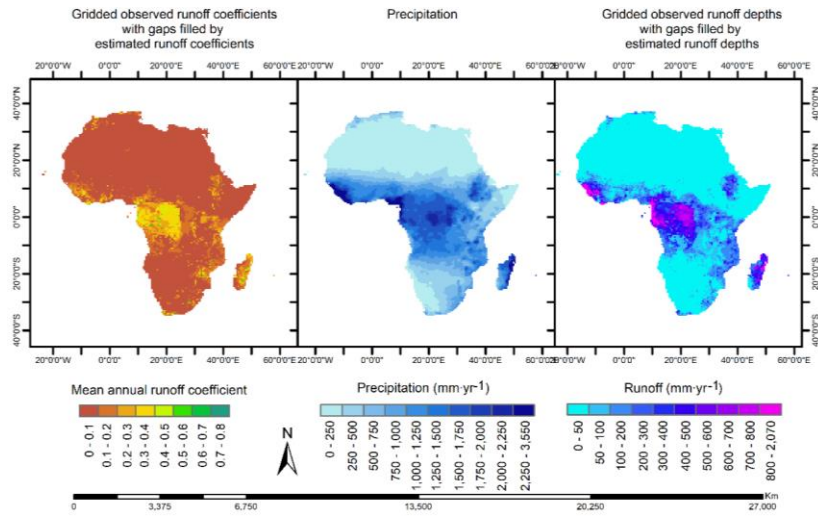
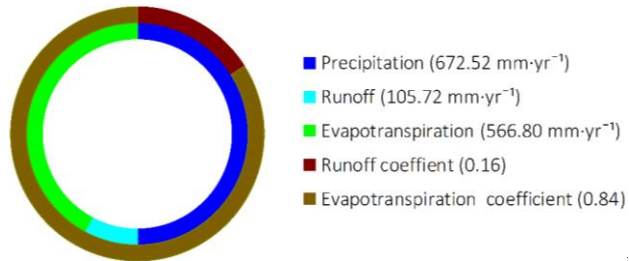


Figure 8. Maps of long-term mean monthly and annual runoff coefficient, precipitation and runoff depths (1901 – 2017/2016).

### 3.1 Precipitation-runoff relationship over the continent of Africa

The zonal statistical analysis at continental level indicates that the runoff (105.7294.9 mm-yr<sup>-1</sup>) counts 16.14% of the long-term mean precipitation (672.52671.88 mm-yr<sup>-1</sup>) and evapotranspiration (566.80576.98 mm-yr<sup>-1</sup>) comprises the remaining 84% of total long-term average rainfall amount (Figure 89).



Formatted: Font: Times New Roman

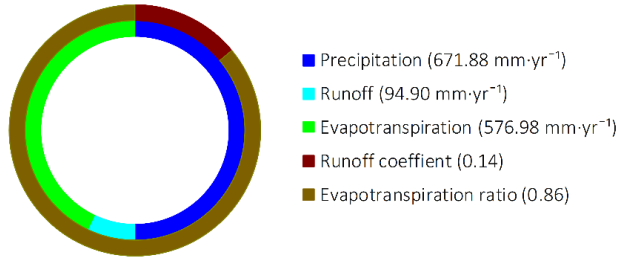
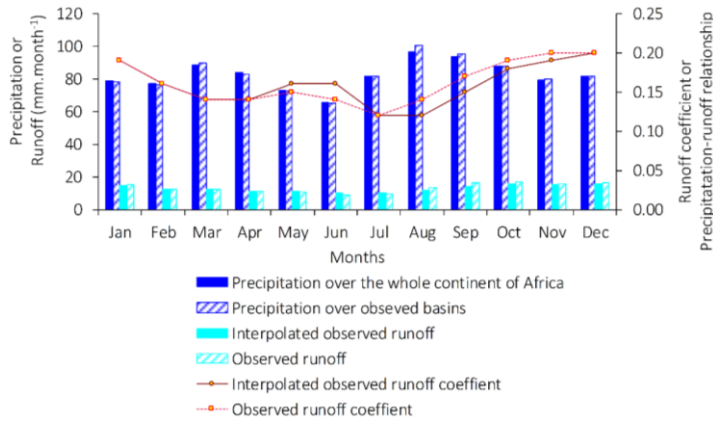


Figure 9. Long-term average annual water balance of Africa (1901 – 2017).

Assessment of the long-term monthly rainfall-runoff relationship revealed that the continent of Africa had experienced the highest and lowest long-term mean precipitation intensities of 70.3347 mm·month<sup>-1</sup> and 44.4513 mm·month<sup>-1</sup> in August and June, respectively. The greatest and smallest long-term mean runoff depths of 11.4620 mm·month<sup>-1</sup> and 5.6419 mm·month<sup>-1</sup> are observed in October/September, and June, respectively. The Figure 10 illustrates that the greatest rainfall-runoff correlation is noticed/recorded in October with a  $R_c = 0.2$ . While, 19, while the lowest  $R_c = 0.1$  are recorded 11 is observed in July whenever  $P = 57.36$  mm·month<sup>-1</sup> and  $R = 6.323$  mm·month<sup>-1</sup> (Fig. 9). The long-term monthly mean observed runoff and runoff coefficient had better agreements with interpolated observed ones. Some minor mismatches observed in May, June, August, September, October and November are due to different mean precipitation estimates from two distinct zones (monitored area and whole continent) (Figure 9/ Figure 10).



Formatted: Font: Times New Roman

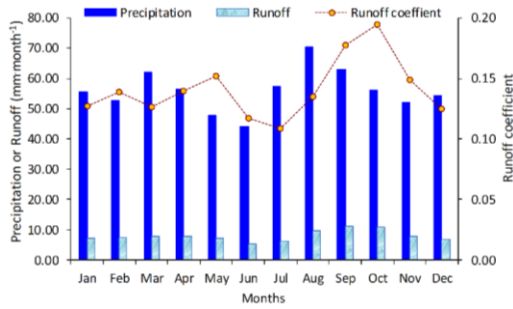
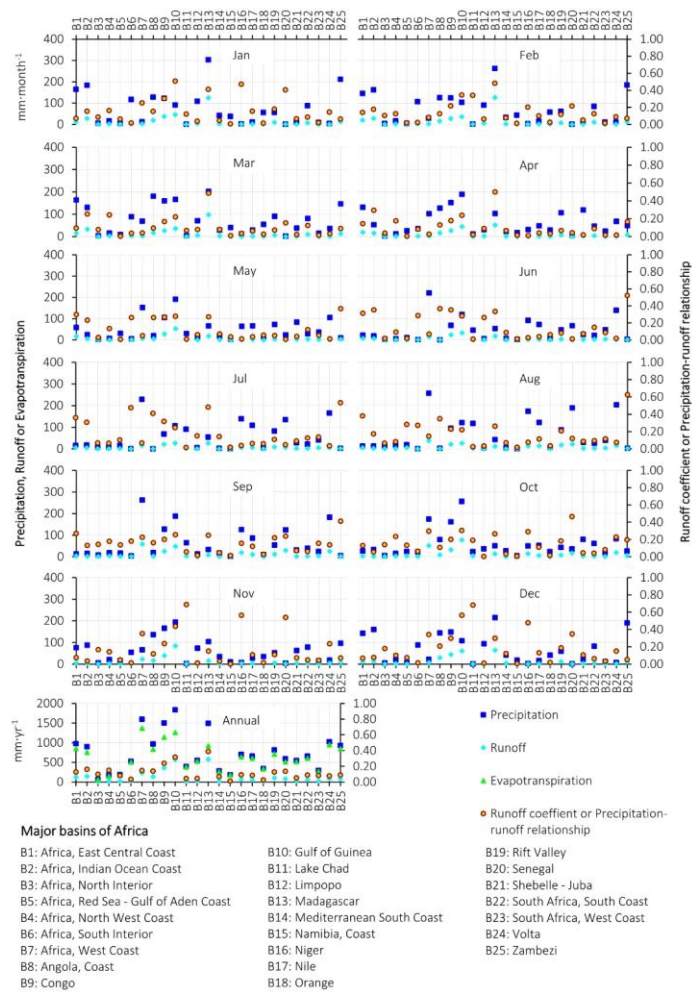


Figure 9.10. Long-term monthly precipitation-runoff relationship over the African continent (1901 – 2017).

### 3.2 Precipitation-runoff relationship within 25 major African basins

Figure 10.11 compares the long-term mean monthly and annual precipitation, interpolated observed runoff, interpolated observed depths, runoff coefficient coefficients, and long-term mean annual evapotranspiration within 25 major African basins (1901 – 2017).

Formatted: Font: Times New Roman



**Figure 9.** Precipitation-runoff relationship within 25 major basins of Africa (1901–2017).

2016). Top eightseven tropical basins out of 25 major African basins that comprised the highest runoff depths > 100 mm-yr<sup>-1</sup> are: Madagascar (575.42 mm-yr<sup>-1</sup>), Gulf of Guinea (573.65594.35 mm-yr<sup>-1</sup>), Madagascar (330.59 mm-yr<sup>-1</sup>), Congo (355.02302.28 mm-yr<sup>-1</sup>), Africa-West Coast (227.68278.76 mm-yr<sup>-1</sup>), Africa-East Central Coast (159.20 mm-yr<sup>-1</sup>), Africa-

Formatted: Font: Times New Roman  
 Formatted: Font: Times New Roman

Indian Ocean Coast (143.89 mm·yr<sup>-1</sup>), Angola-Coast (132.34 mm·yr<sup>-1</sup>), Africa-East-Central-Coast (122.88147.63 mm·yr<sup>-1</sup>), and Rift Valley (101.95 Angola-Coast (111.32 mm·yr<sup>-1</sup>). These Apart from the Volta and Zambezi basins that also have thea relatively high precipitation of 1,028.56 and 917.16 mm·yr<sup>-1</sup>, the above-mentioned basins also comprised of highest long-term annual rainfall intensities among others, ranging from 811.88873.71 mm·yr<sup>-1</sup> to 1,594.88854.64 mm·yr<sup>-1</sup>, and are amongst the top ten basins with the strongest correlation between rainfall and runoff compared to others with a mean runoff coefficient ranging from 0.4312 to 0.3932. The basins with weak precipitation-runoff relationship indicates higher E<sub>T</sub> proportions ratios. Figure 1011 also illustrates the details about monthly precipitation-runoff relationship within 25 major basins of Africa.

Formatted: Font: Times New Roman

Formatted: Font: Times New Roman, English (United Kingdom)

Formatted: Font: Times New Roman

Formatted: Font: Times New Roman, English (United States)

Formatted: Font: Times New Roman, English (United States)

Formatted: Font: Times New Roman

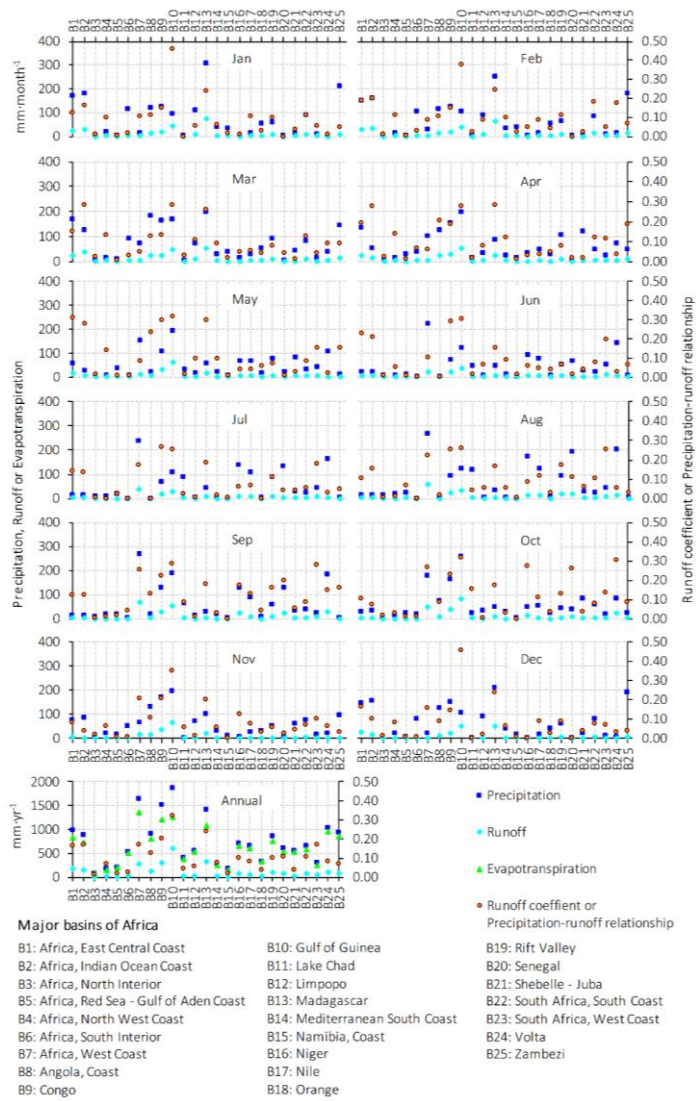


**Figure 11.** Precipitation-runoff relationship within 25 major basins of Africa (1901 – 2016).

### 3.3 Precipitation-runoff relationship within 55 African countries

Figure 112 correlates the long-term mean monthly and annual precipitation ( $P$ ), interpolated observed runoff ( $R$ ), interpolated observed runoff coefficient ( $R_c$ ) and  $RC$ , and long-term mean annual evapotranspiration ( $E_T$ ) during 1901 – 2016 in 55 countries of Africa.  $P$  ranges from 24.3816.54 mm·yr<sup>-1</sup> to 2,820.92788.90 mm·yr<sup>-1</sup>;  $R$  ranges from 4.060.11 mm·yr<sup>-1</sup> to 4,410.68889.78 mm·yr<sup>-1</sup>, in Egypt and MauritiusSierra Leone, respectively;  $R_c$  ranges from 0.04004 in GambiaWestern Sahara to 0.5 Mauritius;  $E_T$  ranges from 20.32 mm·yr<sup>-1</sup>387 in Egypt to 2,099.14 mm·yr<sup>-1</sup> in Sierra LeoneGabon. It should be noticed that, with the highest runoff depths > 300200 mm·yr<sup>-1</sup>. The top 12 countries, including MauritiusSierra Leone, Equatorial Guinea, Gabon, Sierra Leone, Guinea-Bissau, Republic of Congo, Cameroon, Liberia, Comoros, Seychelles, Democratic Republic of the Congo, Madagascar, São Tomé and Príncipe, Republic of Congo, Cameroon, D. R. Congo, Seychelles, and Guinea-BissauMauritius, Burundi, Guinea, and Rwanda are ranked among the top 2016 out of 50 countries that experiences the greatesta relatively strongest rainfall-runoff correlation with runoff coefficients range from 0.4718 to 0.5032. For comparative illustration of the long-term average monthly precipitation, runoff and runoff coefficientcoefficients between 55 countries of Africa, see Figure 112.

Formatted: Font: Times New Roman

Formatted: Font: Times New Roman, English (United States)

Formatted: Font: Times New Roman

Formatted: Font: Times New Roman, Not Superscript/ Subscript

Formatted: Font: Times New Roman

Formatted: Font: Times New Roman

Formatted: Font: Times New Roman

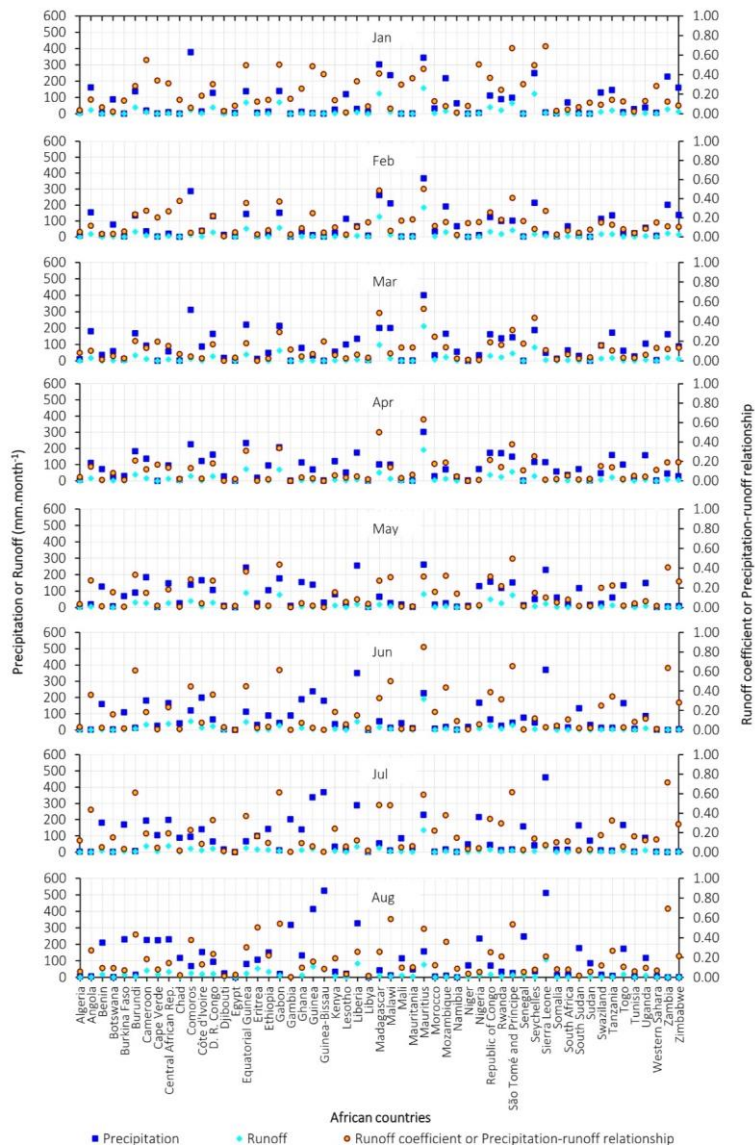
Formatted: Font: Times New Roman, English (United Kingdom), Not Superscript/ Subscript

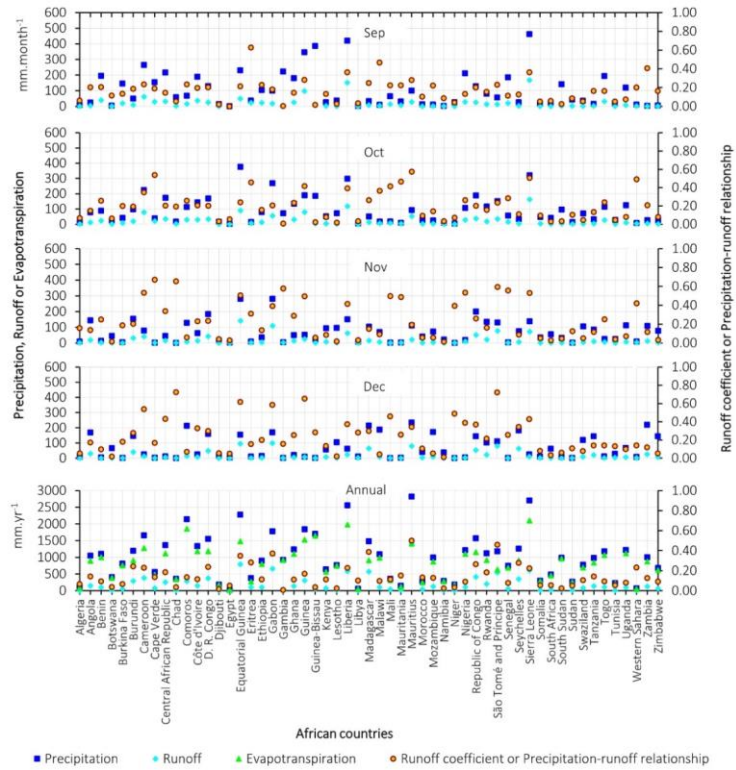
Formatted: Font: Times New Roman, English (United Kingdom)

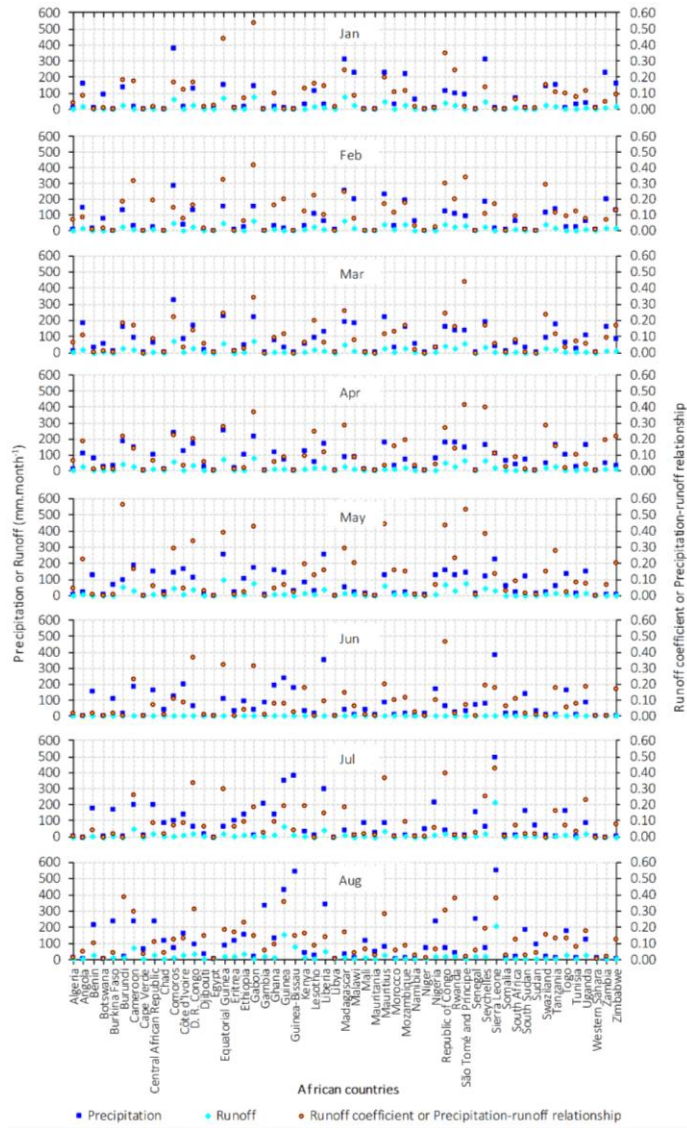
Formatted: Font: Times New Roman

Formatted: Font: Times New Roman, English (United Kingdom)

Formatted: Font: Times New Roman







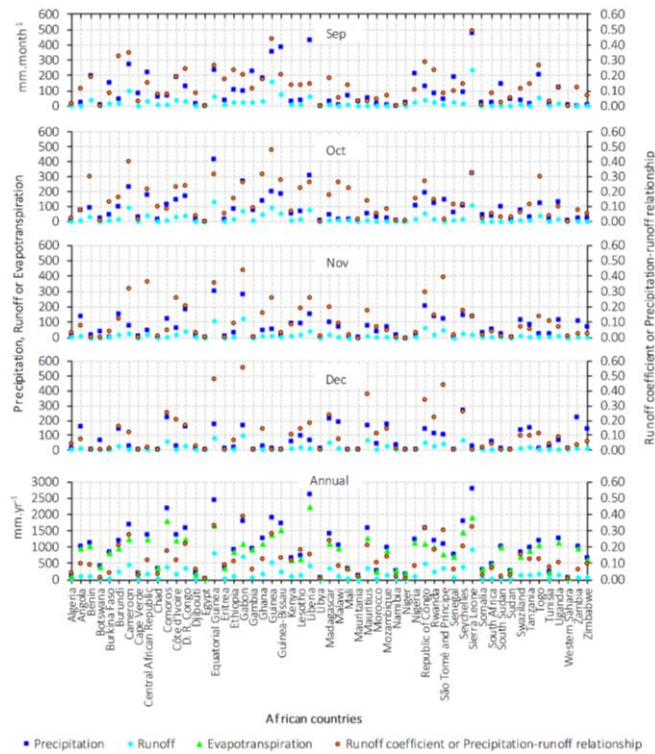


Figure 12. Precipitation-runoff relationship within 55 countries of Africa (1901 – 2017/2016).

#### 4 Discussions

- 5 StreamflowThe streamflow and rain gauging stations are known as a trustable source of reliable data for different hydrological studies (Urroz et al., 2001). The GRDC river discharges and GPCC precipitation datasets have outreaching accuracy for spatial analysis of the precipitation-runoff relationship rather than relying solely on the runoff model-based estimates which are likely associated with huge uncertainties caused by non-error free data and sometimes un-well-constructed models, but the GRDC river discharge data are available with temporal and spatial gaps mostly in low income regions including African countries
- 10 (Figure 13). Obviously, trends in hydrological process are mainly associated with historical climate changes, land-cover change, reservoir storage changes, hydropower releases, and irrigation abstractions which are known to be the primary changing factors affecting the amount of rainwater flow over time (Fekete et al., 2002a). Except, the precipitation datasets

Formatted: Font: Times New Roman

available for the since the beginning of 20<sup>th</sup> century, even before, the other above-mentioned changing runoff controllers are available for the recent decades (i.e.: GRACE data for water storage change analysis were collected since 2002 and good quality land cover maps are available since 1990s). Lack of these data for the earlier decades constrained us to predict the past runoff process. Again, if the earlier runoff discharges are excluded from the long-term runoff calculations, spatial gaps would be increased and bring more challenge for validation.

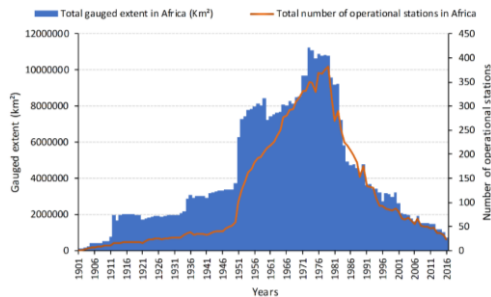


Figure 13. Historical gauged extent and number of operational stations in Africa (1901 – 2016).

A 75.64% of the total observed extent comprise the river discharges with a record of more than 20 years (Figure 3). The scarcity of runoff discharge data is common limitation in runoff prediction at a large extent such as continental scale, but they can provide reasonable results that represent the real world phenomenon (Loucks et al., 2005). The Pre-analysis of the historical changes in annual runoff discharges suggested a linear trend varies between 10% and 40% among the stations which drain the catchments covered by a small extent (8.44% total gauged area). Indeed, a large proportion (91.56%) of the total African gauged area, including the catchments recorded in earlier to recent decades has stations that experienced a minor variance ranging from 0% to 10% which is not a major problem in long-term bases analysis of runoff estimation.

Actually, runoff-related studies are often conducted at a drainage basin scale, but, hydrological studies at the grid and country scales are very useful at national level since each government has own policies for water resource management. Utilization of average basin estimates directly at a country level or any other non-catchment locality seems to be unrealistic. This is the reason why this study highlighted the process of downscaling the basin' observed runoff discharges based on grids' direct runoff contributions to their corresponding basins which helps to include the effect of major runoff controlling factors (i.e.: land cover types, soil characteristics, moisture conditions and precipitation intensities) within different grids sharing the same catchment according to the Natural Resources Conservation Service (NRCS) runoff curve number (CN) method. Even though, the runoff generation process is governed by several environmental factors, but they don't have the same sensitivity and it is still too complicated to incorporate all of them in existing runoff models and methods. In this study, additional factors to those ones utilized in NRCS-CN were considered in fact that there is a considerable dissimilarity of hydrological conditions between separate catchments rather than the grids connected each other within the same catchment. It should be noticed that,

Formatted: Font: Times New Roman  
 Formatted: Font: Times New Roman  
 Formatted: Font: Times New Roman  
 Formatted: ifuvid, Font: Times New Roman

the integration of NRCS-CN in downscaling the runoff discharges do not alter the quantity of observed runoff at a catchment scale, but it redistributes catchment' discharged runoff volumes to their grids according to their respective climate and physical conditions. Some runoff controlling factors such as temperature, topography, etc., are not amongst inputs of the NRCS-CN-based direct runoff prediction, but they also have minor sensitivity a catchment or grid scale with coarse resolution. Runoff discharges were downscaled at 0.5° grid spatial resolution to allow their application at country analysis and facilitate their utilization on estimation over ungauged regions. Gridded observed runoff coefficients were transferred to ungauged areas using inter-gauged and ungauged parameter transfer approach. This is a Geo-spatial analysis technique acceptable for hydrological predictions in ungauged basins (PUB) (Bárdossy, 2007;Blöschl, 2006). This method assumes that two separate catchments can have a similar hydrological process when they have the same range of climatic and physical conditions. Once one of these catchments is observed it can be a source of data to unobserved one. Hydrologic similarity conditions were investigated using the runoff controlling factors selected based on their potential impact highlighted in previous studies. Thus, the efficiency analysis of the approach used to predict the data for filling the gaps suggested that the estimated and observed runoff coefficients have the goodness of fit ( $R^2$ ) ranging from 0.56 to 0.67 for the long-term monthly Rc and 0.78 for the annual mean Rc (Figure 14). These results are within permissible validity limits since an  $R^2 > 0.5$  is considered acceptable for calibration and validation in hydrological modelling (Santhi et al., 2001;Van Liew et al., 2003).

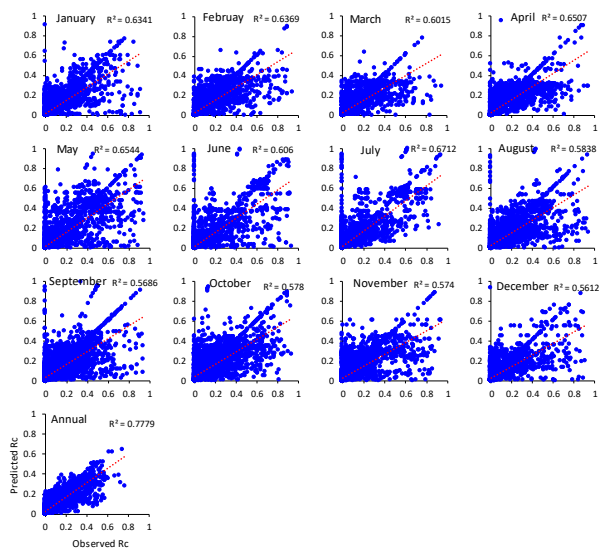


**Figure 14.** Scatter plots with a best-fit line indicating the efficiency of predicted runoff coefficients vs. gridded observed runoff coefficients over the gauged regions of Africa (Figure 7).

It can be concluded that inter-gauged and ungauged basin parameter transfer based on hydrologic similarity is an alternative approach for gaps filling in runoff prediction and it can even perform much better if the input observed runoff discharges do not have a lot of temporal gaps.

Furthermore, the study conducted by the University of New Hampshire-Global Runoff Data Centre (UNH-GRDC):

- 5 “high-resolution fields of global runoff combining observed river discharge and simulated water balances” that has been considered as reference to validate the runoff-related hydrological studies since the beginning of 21<sup>st</sup> century (Fekete et al., 2002; Hong et al., 2007) was compared with the current study based on the latitudinal zones at 1° interval scale (Figure 12). This analysis indicates that the long-term mean (Fekete et al., 2002b; Hong et al., 2007) was compared with the current study based on the latitudinal zones at 1° interval scale (Figure 15). This analysis indicates that the long-term annual mean rainfall
- 10 (1920 – 1980) version 2.01 (Willmott et al., 1998; Fekete et al., 2002) (Willmott C J et al 1998, 1998; Fekete et al., 2002b) that was utilized to simulate the UNH/GRDC composite runoff (Fekete et al., 2002) is roughly matching with the long-term (1901 – 2017) mean annual GPCC precipitation estimated in the current study (Figure 12). (Fekete et al., 2002b) is roughly matching with the long-term (1901 – 2016) mean annual GPCC precipitation estimated in the current study (Figure 15). Our comparative analysis also shows better agreements over the northern hemisphere between 36°N and 14°N, in the southern
- 15 hemisphere between 17°S and 34°S latitudes, and in the equatorial zone laying between 4°N and 8°S. Major differences are between 14°N and 4°N in the northern hemisphere and in the southern hemisphere between 8°S and 17°S latitudes. These differences are possibly due to the UNH/GRDC method that assigned the same runoff depths in observed and unobserved basins that led to overestimation of the runoff in drylands of Australia and Africa (Fekete et al., 2002). It should be noted that the interpolation method of observed runoff coefficient under consideration of environmental characteristics (land use and
- 20 cover types, slope, soil texture classes, surface temperature and precipitation) has improved of both runoff coefficient and runoff over unobserved African regions rather than assuming similar runoff depths to different catchments with different environmental characteristics, and gridded runoff depth that was estimated by considering rainfall factor alone (Fekete et al., 2002). The latitudinal profile analysis revealed that on the 2°S latitude is the runoff hotspot region of Africa with higher mean R depth (387.65 mm·yr<sup>-1</sup>) and P (1,422.77 mm·yr<sup>-1</sup>), and a relatively strongest P-R correlation with Rc of 0.27, followed by
- 25 the 1°S latitude zone with the R of 383.87 mm·yr<sup>-1</sup>, P of 1,504.47 mm·yr<sup>-1</sup>, and Rc of 0.26, and as well equatorial zone at 0° latitude with a mean R of 379.99 mm·yr<sup>-1</sup>, P of 1,490.18 mm·yr<sup>-1</sup>, and Rc of 0.25.

Formatted: Font: Times New Roman

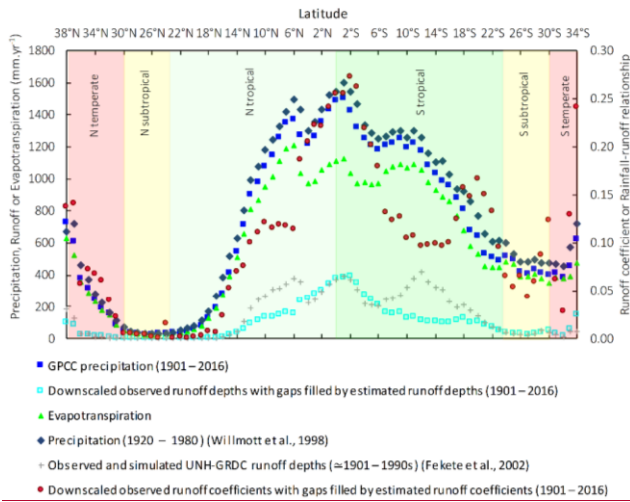
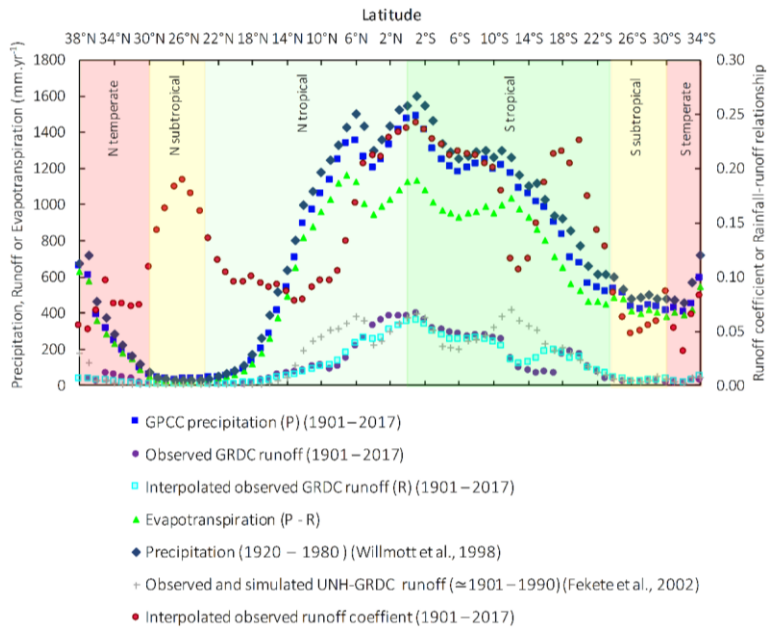


**Figure 15.** Comparison of the precipitation-runoff relationship between the UNH-GRDC (Fekete et al., 2002) and the present study.

The latitudinal profile analysis revealed that 1°S latitude is the most hotspot region of Africa for both high mean annual rainfall intensity (1,486 mm·yr<sup>-1</sup>), and runoff depth (357.26 mm·yr<sup>-1</sup>), followed by the equatorial zone at 0° latitude with a mean annual rainfall intensity of 1,466.46 mm·yr<sup>-1</sup>, runoff depth of 346.66 mm·yr<sup>-1</sup>, highest runoff coefficient value of 0.24 for both 1°S and equatorial zone (0° latitude). These latitudinal zones also comprised of the highest evapotranspiration rates ranging between 1,119.8 mm·yr<sup>-1</sup> and 1,157.24 mm·yr<sup>-1</sup>. This might be one of the remarkable proofs showing good estimates of the present study based on the well known distribution of precipitation across different latitudinal climatic zones (Peel et al., 2007).

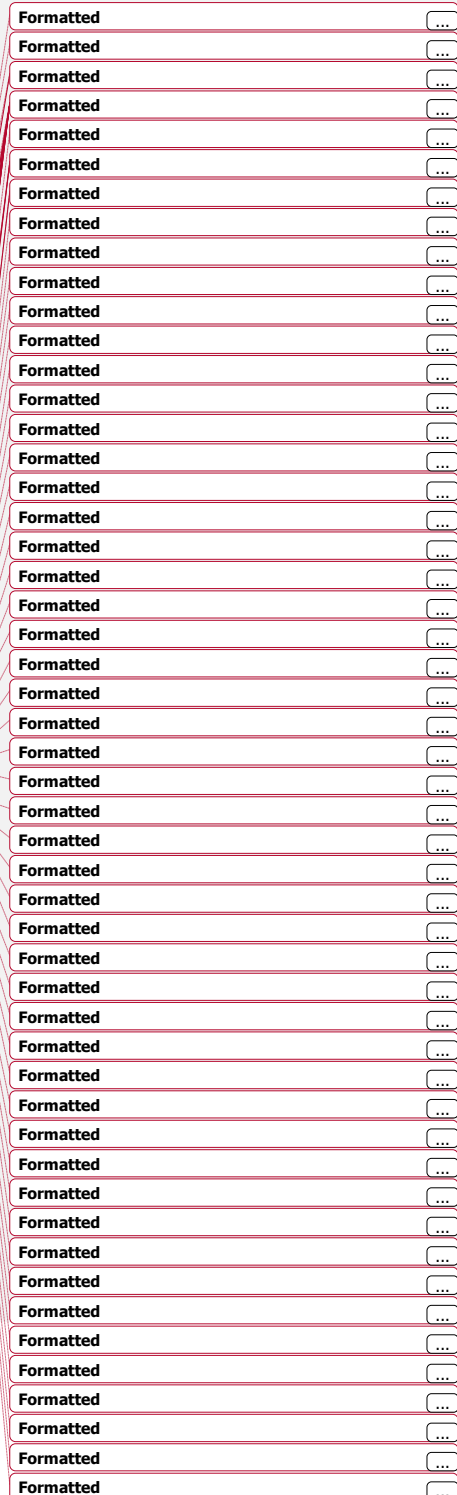
Comparison of the precipitation-runoff relationship between the UNH-GRDC (Fekete et al., 2002b) and the present study.

Based on the following six latitudinal climate zones; northern (N) tropical (0°Equator ≤ latitude ≤ 23.4°N), southern (S) tropical (23.4°S ≤ latitude < 0°Equator), N subtropics (23.4°N ≤ latitude ≤ 30°N), S subtropics (23.4°S ≤ latitude ≤ 30°S), N temperate (30°N < latitude ≤ 72°N), and S temperate (30°S < latitude ≤ 72°S); (Peel et al., 2007), the long-term annual mean of the water balance's variables, including precipitation (P), evapotranspiration (E<sub>T</sub>), interpolated-observed runoff (R) and their corresponding interpolated-observed runoff coefficient coefficients (R<sub>C</sub>) for the period of 117116 years (1901 – 20172016) were estimated and presented in Table 24, to provide tangible statistics corresponding to Figure 1215.

**Table 4.** Long-term annual water balance and runoff coefficient coefficients within the African latitudinal climatic zones (1901 – 20172016).

Latitudinal climatic zones	% area Africa	P (mm·yr <sup>-1</sup> )	E <sub>T</sub> (mm·yr <sup>-1</sup> )	R (mm·yr <sup>-1</sup> )	R <sub>C</sub>
<b>Tropical</b>	<b>75</b>	<b>835836.36</b>	<b>699713.70</b>	<b>136122.66</b>	<b>0.1615</b>
N tropical	48	703708.94	607615.72	9693.22	0.1413
S tropical	26	1,076070.13	865893.45	214176.68	0.2017
<b>Subtropics</b>	<b>17</b>	<b>156146.23</b>	<b>143138.03</b>	<b>138.20</b>	<b>0.0806</b>
N subtropical	13	3728.35	3428.22	60.13	0.1600
S subtropical	5	468455.27	437425.91	3429.36	0.0706
<b>Temperate zones</b>	<b>8</b>	<b>261257.34</b>	<b>243236.94</b>	<b>1820.40</b>	<b>0.0708</b>
N temperate	6	219207.51	195193.79	1513.72	0.07
S temperate	2	432423.94	406381.21	2642.73	0.0610

Because of the Saharan desert located in northern Africa, the northern tropical and temperate zones have lower mean annual precipitation and runoff compared to southern tropical and temperate zones. Compared to the tropical zone, subtropics and temperate zones of Africa had low rainfall and runoff amounts (Figure 12 and Table 2), which expose them to water scarcity problem and less rainfall runoff related disasters. The problem of insufficient water resource in drylands and semi-humid regions can be managed through the use of groundwater, minimization of water losses, establishment of dams, inter-basins water transfer, wastewater reuse, and surface water desalination instead of relying on unmodernized water supply technologies that are no longer meeting the water demand for our contemporary development associated with fast population



growth. Compared to the tropical zone, subtropical and temperate zones of Africa have low rainfall and runoff amounts (Figure 15 and Table 4), which may expose them to the water scarcity (Maliva and Missimer, 2012). The countries and basins located in the tropical zone are often prone to a higher precipitation intensity which produces huge runoff volumes enough for underground and surface water replenishment. While, excessive surface waterflow induces significant damages which require adequate strategies by promoting practical, however, some time causing stormwater management systems (e.g.: forestation, different types of terraces and dams, etc.) that have potential ability to curb the movement and effects of surface water runoffs-related disasters (Ponette-González et al., 2015; Karamage et al., 2017b).

## 5 Conclusions

The present study investigated the spatial relationship between precipitation and runoff using the runoff coefficient as the measurement indicator, estimated from the long-term monthly runoff calculated based on the Global Runoff Data Centre (GRDC)'s streamflow records and Global Precipitation Climatology Centre (GPCC) rainfall data for a temporal period of 117 years (1901–2017) within monitored basins covering  $\approx 41.4\%$  of the total African continent. The interpolation method of observed runoff coefficient directed by the ancillary data (potential runoff coefficient, land surface temperature, and precipitation) that affect the runoff generation process has improved the estimation of runoff coefficient and runoff depths in ungauged basins. Thus, this study provides insightful hydrological information on the precipitation-runoff relationship at three spatial scales, including the whole continent, 25 major basins and 55 African countries which could raise the awareness to a wide range of relevant stakeholders. This study also suggested that the problem of water scarcity in drylands and semi-humid region can be handled through the use of groundwater, minimization of water losses, establishment of dams, inter-basins water transfer, wastewater reuse, and water desalination technologies. The tropical stormwater runoffs require suitable water management programs such as for example forestation, establishment of different types of terraces and dams, etc. in order to minimize the waterflow-related disasters.

This study has highlighted step by step how the Natural Resources Conservation Service (NRCS) runoff curve number (CN) can be a prominent proxy for the basin's river discharge downscaling at a grid scale which can be reasonably utilized on non-catchment regional studies. This approach helped us to produce gridded long-term monthly runoff depths and coefficients datasets used to analyze the spatial relationship between precipitation and runoff over all 55 countries and 25 major drainage basins covering the whole continent of Africa. The Global Runoff Data Centre (GRDC)'s streamflow records available for 535 catchments covering  $\approx 47.43\%$  of the total African continent became a source of information for predicting the P-R correlation over ungauged regions based on the inter-gauged and ungauged parameter transfer approach and spatial hydrologic similarity analysis assessed using the key runoff controlling factors including antecedent moisture condition (AMC), NRCS-CN, terrestrial water storage, temperature, topographic wetness index (TWI), and slope. Both higher runoff depths and strong P-R correlation were observed in the tropical humid regions due to their intensive precipitation more than in subtropical and temperate zones. This study suggests the need for rehabilitation awareness of operational stream gauging stations and

Formatted: Font: Times New Roman

Formatted: Font: Times New Roman, English (United States)

Formatted: Font: Times New Roman

establishment of new ones where they are necessary to make sure streamflow are regularly and widely recorded in different catchments of Africa to provide sufficient update data required for accurate water resource planning.

**Acknowledgments:** Many thanks to the editor and anonymous referees for the insightful comments that helped us to improve the quality of this manuscript. This study was supported by: (a) the Chinese Academy of Sciences and the World Academy of Sciences (CAS-TWAS) President's PhD Fellowship Program, and (b) the Sino-Africa Joint Research Centre, Chinese Academy of Sciences (No. SAJC201609).

Formatted: Font: Times New Roman

Formatted: Font: Times New Roman

Formatted: Font: Times New Roman

## References

Ahmed, K., Shahid, S., and Harun, S. B.: Spatial interpolation of climatic variables in a predominantly arid region with complex topography, *Environment Systems and Decisions*, 34, 555-563, 2014.

10 Becker, A., Finger, P., Meyer-Christoffer, A., Rudolf, B., Schamm, K., Schneider, U., and Ziese, M.: A description of the global land-surface precipitation data products of the Global Precipitation Climatology Centre with sample applications including centennial (trend) analysis from 1901–present, *Earth System Science Data*, 5, 71-99, 2013.

Blume, T., Zehe, E., and Bronstert, A.: Rainfall—runoff response, event-based runoff coefficients and hydrograph separation, *Hydrological Sciences Journal*, 52, 843-862, 2007.

15 Brown, J. L., Bennett, J. R., and French, C. M.: SDMtoolbox 2.0: the next-generation Python-based GIS toolkit for landscape genetic, biogeographic and species distribution model analyses, *PeerJ*, 5, e4095, 2017.

Cervigni, R., and Morris, M.: Confronting Drought in Africa's Drylands: Opportunities for Enhancing Resilience, World Bank Publications, 2016.

20 Chen, L., Liu, C., Li, Y., and Wang, G.: Impacts of climatic factors on runoff coefficients in source regions of the Huanghe River, *Chinese Geographical Science*, 17, 047-055, 2007.

Clover, J.: Food security in sub-saharan Africa: feature, *African security review*, 12, 5-15, 2003.

Cohen, J. E., and Small, C.: Hypsographic demography: the distribution of human population by altitude, *Proceedings of the National Academy of Sciences*, 95, 14009-14014, 1998.

Corlett, R. T.: Where are the Subtropics?, *Biotropica*, 45, 273-275, 2013.

25 Cosgrove, W. J., and Loucks, D. P.: Water management: Current and future challenges and research directions, *Water Resources Research*, 51, 4823-4839, 10.1002/2014wr016869, 2015.

Danielson, J. J., and Gesch, D. B.: Global multi-resolution terrain elevation data 2010 (GMTED2010), US Geological Survey 2331-1258, 2011.

30 Dewitte, O., Jones, A., Spaargaren, O., Breuning-Madsen, H., Brossard, M., Dampha, A., Deekers, J., Gallali, T., Hallett, S., and Jones, R.: Harmonisation of the soil map of Africa at the continental scale, *Geoderma*, 211, 138-153, 2013.

Edwards, P. J., Williard, K. W., and Schoonover, J. E.: Fundamentals of watershed hydrology, *Journal of Contemporary Water Research & Education*, 154, 3-20, 2015.

ESA-CCI: Land Cover CCI PRODUCT USER GUIDE VERSION 2.0, DOCUMENT REF: CCI-LC-PUGV2: [http://maps.elic.ucl.ac.be/CCI/viewer/download/ESACCI-LC-Ph2-PUGv2\\_2.0.pdf](http://maps.elic.ucl.ac.be/CCI/viewer/download/ESACCI-LC-Ph2-PUGv2_2.0.pdf), access: 15 January, 2017.

- FAO: Hydrological basins in Africa (Derived from HydroSHEDS).<http://www.fao.org/geonetwork/srv/en/main.search?any=awrd&themekey=%22watersheds%22,2009>, access: 20 January, 2018.
- Fekete, B. M., Vörösmarty, C. J., and Grabs, W.: High-resolution fields of global runoff combining observed river discharge and simulated water balances, *Global Biogeochemical Cycles*, 16, 2002.
- 5 Fernandez-Iglesias, C. P., Porporato, A., Laio, F., and Rodriguez-Iturbe, I.: The ecohydrological role of soil texture in a water-limited ecosystem, *Water Resources Research*, 37, 2863–2872, 2001.
- Goudie, A.: *The human impact on the natural environment*, MIT press, 2000.
- GRDC: The Global Runoff Data Centre, 56068 Koblenz, Germany.[http://www.bafg.de/GRDC/EN/02\\_srves/21\\_tmsrs/riverdischarge\\_node.html](http://www.bafg.de/GRDC/EN/02_srves/21_tmsrs/riverdischarge_node.html), 2018, access: 25 January, 2018.
- 10 Harris, I., Jones, P., Osborn, T., and Lister, D.: Updated high-resolution grids of monthly climatic observations—the CRU-TS3.10 Dataset, *International Journal of Climatology*, 34, 623–642, 2014.
- Hengl, T., de Jesus, J. M., MacMillan, R. A., Batjes, N. H., Heuvelink, G. B., Ribeiro, E., Samuel-Rosa, A., Kempen, B., Leenaars, J. G., and Walsh, M. G.: SoilGrids1km—global soil information based on automated mapping, *PLoS One*, 9, e105992, 2014.
- Hengl, T., Heuvelink, G. B., Kempen, B., Leenaars, J. G., Walsh, M. G., Shepherd, K. D., Sila, A., MacMillan, R. A., de Jesus, J. M., and  
15 Tamene, L.: Mapping soil properties of Africa at 250 m resolution: random forests significantly improve current predictions, *PLoS one*, 10, e0125814, 2015.
- Hong, Y., Adler, R. F., Hossain, F., Curtis, S., and Huffman, G. J.: A first approach to global runoff simulation using satellite rainfall estimation, *Water Resources Research*, 43, 2007.
- Huang, B., and Hu, T.: Spatial Interpolation of Rainfall Based on DEM, in: *Advances in Water Resources and Hydraulic Engineering*, Springer, 77–81, 2009.
- 20 Kadioglu, M., and ŞEN, Z.: Monthly precipitation-runoff polygons and mean runoff coefficients, *Hydrological Sciences Journal*, 46, 3–11, 2001.
- Karamage, F., Zhang, C., Ndayisaba, F., Nahayo, L., Kayiranga, A., Omifolaji, J. K., Shao, H., Umuhoza, A., Nsengiyumva, J. B., and Liu, T.: The need for awareness of drinking water loss reduction for sustainable water resource management in Rwanda, *Journal of Geoscience and Environment Protection*, 4, 74, 2016.
- 25 Karamage, F., Zhang, C., Fang, X., Liu, T., Ndayisaba, F., Nahayo, L., Kayiranga, A., and Nsengiyumva, J. B.: Modeling rainfall-runoff response to land use and land cover change in Rwanda (1990–2016), *Water*, 9, 147, 2017a.
- Karamage, F., Zhang, C., Liu, T., Maganda, A., and Isabwwe, A.: Soil Erosion Risk Assessment in Uganda, *Forests*, 8, 52, 2017b.
- Liu, Y., and De Smedt, F.: WetSpa extension, a GIS-based hydrologic model for flood prediction and watershed management, *Vrije*  
30 *Universiteit Brussel, Belgium*, 1–108, 2004.
- Long, D., Longuevergne, L., and Seanlon, B. R.: Uncertainty in evapotranspiration from land surface modeling, remote sensing, and GRACE satellites, *Water Resources Research*, 50, 1131–1151, 2014.
- Loucks, D., Van Beek, E., Stedinger, J., Dijkman, J., and Villars, M.: Model sensitivity and uncertainty analysis, *Water resources systems planning and management*, 255–290, 2005.
- 35 Maliva, R., and Missimer, T.: *Arid lands water evaluation and management*, Springer Science & Business Media, 2012.
- Mawere, M.: *Underdevelopment, Development and the Future of Africa*, Langaa Rpcig, 2017.
- Messer, E., Cohen, M. J., and Marchione, T.: Conflict: A cause and effect of hunger, *Environmental Change and Security Project Report*, 7, 1–16, 2001.

- Moucha, R., and Forte, A. M.: Changes in African topography driven by mantle convection, *Nature Geoscience*, 4, 707, 2011.
- Oyebande, L.: Water problems in Africa—how can the sciences help?, *Hydrological Sciences Journal*, 46, 947-962, 2001.
- Paul, J. D., Roberts, G. G., and White, N.: The African landscape through space and time, *Tectonics*, 33, 898-935, 2014.
- Peel, M. C., Finlayson, B. L., and McMahon, T. A.: Updated world map of the Köppen-Geiger climate classification, *Hydrology and earth system sciences discussions*, 4, 439-473, 2007.
- Penman, J., Gytarsky, M., Hiraishi, T., Krug, T., Kruger, D., Pipatti, R., Buendia, L., Miwa, K., Ngara, T., and Tanabe, K.: Good practice guidance for land use, land use change and forestry, *Good practice guidance for land use, land use change and forestry*, 2003.
- Ponette-González, A. G., Brauman, K. A., Marín-Spiotta, E., Farley, K. A., Weathers, K. C., Young, K. R., and Curran, L. M.: Managing water services in tropical regions: From land cover proxies to hydrologic fluxes, *Ambio*, 44, 367-375, 2015.
- Sanabria, L., Qin, X., Li, J., Cechet, R., and Lucas, C.: Spatial interpolation of McArthur's forest fire danger index across Australia: observational study, *Environmental modelling & software*, 50, 37-50, 2013.
- Sayre, and Pulley, A.: *Africa, Twenty-First Century Books*, 1999.
- Schamm, K., Ziese, M., Becker, A., Finger, P., Meyer-Christoffer, A., Schneider, U., Schröder, M., and Stender, P.: Global gridded precipitation over land: A description of the new GPCP First Guess Daily product, *Earth System Science Data*, 6, 49-60, 2014.
- Sriwongsitanon, N., and Taesombat, W.: Effects of land cover on runoff coefficient, *Journal of Hydrology*, 410, 226-238, 2011.
- Terakawa, A.: *Hydrological data management: Present state and trends*, Secretariat of the World Meteorological Organization, 2003.
- UN-DESA: United Nations, Department of Economic and Social Affairs, Population Division (2017). *World Population Prospects: The 2017 Revision, Key Findings and Advance Tables*. ESA/P/WP/248. <https://esa.un.org/unpd/wpp/Publications/>, 2017, access: 20 January, 2018.
- UNISDR: *Global Assessment Report on Disaster Risk Reduction (GAR 2011)*. <https://www.preventionweb.net/english/hyogo/gar/>, 2011, access: 17 February, 2018.
- UNISDR: *Global Assessment Report on Disaster Risk Reduction (GAR 2015)*. <https://www.preventionweb.net/english/hyogo/gar/>, 2015, access: 17 February, 2018.
- Urroz, G., Leines, R. C., Perret, G. L., Holland, J. M., and Hunsaker, B. E.: *Development of a Low-cost, Self-calibrating Stream Gaging Station*, 2001.
- Walkenbach, J.: *Excel 2010 power programming with VBA*, John Wiley & Sons, 2010.
- Weng, Q.: Modeling urban growth effects on surface runoff with the integration of remote sensing and GIS, *Environmental management*, 28, 737-748, 2001.
- Global Air Surface temperature and Precipitation Climatologies, by : Cort J. Willmott, Kenji Matsuura and David R. Legates (Center for Climate Research, University of Delaware), version 2.01, November 1998: <https://rda.uear.edu/datasets/ds236.0/>, access: 10 January, 2018.
- Yang, L., Sun, G., Zhi, L., and Zhao, J.: Negative soil moisture-precipitation feedback in dry and wet regions, *Scientific reports*, 8, 4026, 2018.
- Abdi, A. M., Boke-Olén, N., Tenenbaum, D. E., Tagesson, T., Cappelerae, B., and Ardö, J.: Evaluating water controls on vegetation growth in the semi-arid Sahel using field and Earth observation data, *Remote Sensing*, 9, 294, 2017.
- Anja, M.-C., Andreas, B., Peter, F., Udo, S., and Markus, Z.: *GPCC Climatology Version 2018 at 0.5°: Monthly Land-Surface Precipitation Climatology for Every Month and the Total Year from Rain-Gauges built on GTS-based and Historical Data*. DOI: 10.5676/DWD\_GPCC/CLIM\_M\_V2018\_050, 2018.

- Bárdossy, A.: Calibration of hydrological model parameters for ungauged catchments, *Hydrology and Earth System Sciences Discussions*, 11, 703-710, 2007.
- Beck, H. E., de Jeu, R. A., Schellekens, J., van Dijk, A. I., and Bruijnzeel, L. A.: Improving curve number based storm runoff estimates using soil moisture proxies, *IEEE Journal of selected topics in applied earth observations and remote sensing*, 2, 250-259, 2009.
- 5 BEVEN, K. J., and Kirkby, M. J.: A physically based, variable contributing area model of basin hydrology/Un modèle à base physique de zone d'appel variable de l'hydrologie du bassin versant, *Hydrological Sciences Journal*, 24, 43-69, 1979.
- Blöschl, G.: Rainfall-runoff modeling of ungauged catchments, *Encyclopedia of hydrological sciences*, 2006.
- Blume, T., Zehe, E., and Bronstert, A.: Rainfall—runoff response, event-based runoff coefficients and hydrograph separation, *Hydrological Sciences Journal*, 52, 843-862, 2007.
- 10 Brown, J. L., Bennett, J. R., and French, C. M.: SDMtoolbox 2.0: the next generation Python-based GIS toolkit for landscape genetic, biogeographic and species distribution model analyses, *PeerJ*, 5, e4095, 2017.
- Cervigni, R., and Morris, M.: Confronting Drought in Africa's Drylands: Opportunities for Enhancing Resilience, *World Bank Publications*, 2016.
- 15 Chen, L., Liu, C., Li, Y., and Wang, G.: Impacts of climatic factors on runoff coefficients in source regions of the Huanghe River, *Chinese Geographical Science*, 17, 047-055, 2007.
- Chiew, F., Zheng, H., and Potter, N.: Rainfall-Runoff Modelling Considerations to Predict Streamflow Characteristics in Ungauged Catchments and under Climate Change, *Water*, 10, 1319, 2018.
- Clover, J.: Food security in sub-saharan Africa: feature, *African security review*, 12, 5-15, 2003.
- 20 Cook, K. H., and Vizy, E. K.: Detection and analysis of an amplified warming of the Sahara Desert, *Journal of Climate*, 28, 6560-6580, 2015.
- Cosgrove, W. J., and Loucks, D. P.: Water management: Current and future challenges and research directions, *Water Resources Research*, 51, 4823-4839, 10.1002/2014wr016869, 2015.
- Cronsey, R.: Urban hydrology for small watersheds, *US Dept. of Agriculture, Soil Conservation Service, Engineering Division*, 1986.
- 25 Dewitte, O., Jones, A., Spaargaren, O., Breuning-Madsen, H., Brossard, M., Dampah, A., Deckers, J., Gallali, T., Hallett, S., and Jones, R.: Harmonisation of the soil map of Africa at the continental scale, *Geoderma*, 211, 138-153, 2013.
- Edwards, P. J., Williard, K. W., and Schoonover, J. E.: Fundamentals of watershed hydrology, *Journal of Contemporary Water Research & Education*, 154, 3-20, 2015.
- Engineers, U. A. C.: Hydrologic modeling system (HEC-HMS) application guide: version 3.1. 0, *Institute for Water Resources, Davis*, 2008.
- 30 Land Cover CCI PRODUCT USER GUIDE VERSION 2.0. DOCUMENT REF: CCI-LC-PUGV2: [http://maps.elie.ucl.ac.be/CCI/viewer/download/ESACCI-LC-Ph2-PUGv2\\_2.0.pdf](http://maps.elie.ucl.ac.be/CCI/viewer/download/ESACCI-LC-Ph2-PUGv2_2.0.pdf), access: 15 January, 2017.
- Hydrological basins in Africa (Derived from HydroSHEDS). <http://www.fao.org/geonetwork/srv/en/main.search?any=awrd&themekey=%22watersheds%22>, 2009.
- Fekete, B. M., Vörösmarty, C. J., and Grabs, W.: High-resolution fields of global runoff combining observed river discharge and simulated water balances, *Global Biogeochemical Cycles*, 16, 15-11-15-10, 2002a.
- 35 Fekete, B. M., Vörösmarty, C. J., and Grabs, W.: High-resolution fields of global runoff combining observed river discharge and simulated water balances, *Global Biogeochemical Cycles*, 16, 2002b.
- Fernandez-Illescas, C. P., Porporato, A., Laio, F., and Rodriguez-Iturbe, I.: The ecohydrological role of soil texture in a water-limited ecosystem, *Water Resources Research*, 37, 2863-2872, 2001.
- GADM: Global Administrative Areas (GADM), version 2.8, November 2015. [www.gadm.org](http://www.gadm.org), 2015.
- 40 Goudie, A.: The human impact on the natural environment, *MIT press*, 2000.
- The Global Runoff Data Centre, 56068 Koblenz, Germany. [http://www.bafg.de/GRDC/EN/02\\_srvcs/21\\_tmsrs/riverdischarge\\_node.html](http://www.bafg.de/GRDC/EN/02_srvcs/21_tmsrs/riverdischarge_node.html), 2018.
- Halwatura, D., and Najim, M.: Application of the HEC-HMS model for runoff simulation in a tropical catchment, *Environmental modelling & software*, 46, 155-162, 2013.
- 45 Harris, L., Jones, P., Osborn, T., and Lister, D.: Updated high-resolution grids of monthly climatic observations—the CRU TS3. 10 Dataset, *International Journal of Climatology*, 34, 623-642, 2014.
- Hawkins, R. H.: Asymptotic determination of runoff curve numbers from data, *Journal of Irrigation and Drainage Engineering*, 119, 334-345, 1993.
- Heggen, R. J.: Normalized antecedent precipitation index, *Journal of hydrologic Engineering*, 6, 377-381, 2001.
- 50 Hengl, T., de Jesus, J. M., MacMillan, R. A., Batjes, N. H., Heuvelink, G. B., Ribeiro, E., Samuel-Rosa, A., Kempen, B., Leenaars, J. G., and Walsh, M. G.: SoilGrids1km—global soil information based on automated mapping, *PLoS One*, 9, e105992, 2014.
- Hengl, T., Heuvelink, G. B., Kempen, B., Leenaars, J. G., Walsh, M. G., Shepherd, K. D., Sila, A., MacMillan, R. A., de Jesus, J. M., and Tamene, L.: Mapping soil properties of Africa at 250 m resolution: random forests significantly improve current predictions, *PLoS one*, 10, e0125814, 2015.
- 55 Hong, Y., Adler, R. F., Hossain, F., Curtis, S., and Huffman, G. J.: A first approach to global runoff simulation using satellite rainfall estimation, *Water Resources Research*, 43, 2007.

- Jaleta, D., Mbilinyi, B. P., Mahoo, H. F., and Lemenih, M.: Effect of Eucalyptus expansion on surface runoff in the central highlands of Ethiopia, *Ecological Processes*, 6, 1, 2017.
- Kadioglu, M., and ŞEN, Z.: Monthly precipitation-runoff polygons and mean runoff coefficients, *Hydrological Sciences Journal*, 46, 3-11, 2001.
- 5 Karamage, F., Zhang, C., Ndayisaba, F., Nahayo, L., Kayiranga, A., Omifolaji, J. K., Shao, H., Umuhoza, A., Nsengiyumva, J. B., and Liu, T.: The need for awareness of drinking water loss reduction for sustainable water resource management in Rwanda, *Journal of Geoscience and Environment Protection*, 4, 74, 2016.
- Karamage, F., Zhang, C., Fang, X., Liu, T., Ndayisaba, F., Nahayo, L., Kayiranga, A., and Nsengiyumva, J. B.: Modeling rainfall-runoff response to land use and land cover change in Rwanda (1990–2016), *Water*, 9, 147, 2017a.
- 10 Karamage, F., Zhang, C., Liu, T., Maganda, A., and Isabwe, A.: Soil Erosion Risk Assessment in Uganda, *Forests*, 8, 52, 2017b.
- Knisel, W., and Douglas-Mankin, K.: CREAMS/GLEAMS: Model use, calibration, and validation, *Transactions of the ASABE*, 55, 1291-1302, 2012.
- Kohler, M. A., and Linsley, R. K.: Predicting the runoff from storm rainfall, US Department of Commerce, Weather Bureau Washington, DC, 1951.
- 15 Lehner, B., Verdin, K., and Jarvis, A.: New global hydrography derived from spaceborne elevation data, *Eos, Transactions American Geophysical Union*, 89, 93-94, 2008.
- Lim, K. J., Engel, B. A., Muthukrishnan, S., and Harbor, J.: EFFECTS OF INITIAL ABSTRACTION AND URBANIZATION ON ESTIMATED RUNOFF USING CN TECHNOLOGY 1, *JAWRA Journal of the American Water Resources Association*, 42, 629-643, 2006.
- 20 Liu, T., Yan, H., and Zhai, L.: Extract relevant features from DEM for groundwater potential mapping, *The International Archives of Photogrammetry, Remote Sensing and Spatial Information Sciences*, 40, 113, 2015.
- Liu, Y., and De Smedt, F.: WetSpa extension, a GIS-based hydrologic model for flood prediction and watershed management, *Vrije Universiteit Brussel, Belgium*, 1-108, 2004.
- 25 Long, D., Longuevergne, L., and Scanlon, B. R.: Uncertainty in evapotranspiration from land surface modeling, remote sensing, and GRACE satellites, *Water Resources Research*, 50, 1131-1151, 2014.
- Loucks, D., Van Beek, E., Stedinger, J., Dijkman, J., and Villars, M.: Model sensitivity and uncertainty analysis, *Water resources systems planning and management*, 255-290, 2005.
- Mahmoud, S. H.: Investigation of rainfall-runoff modeling for Egypt by using remote sensing and GIS integration, *Catena*, 120, 111-121, 2014.
- 30 Maliva, R., and Missimer, T.: Arid lands water evaluation and management, Springer Science & Business Media, 2012.
- Markus, Z., Armin, R.-S., Andreas, B., Peter, F., Anja, M.-C., and Udo, S.: GPCC Full Data Daily Version 2018 at 1.0°: Daily Land-Surface Precipitation from Rain-Gauges built on GTS-based and Historic Data, DOI: 10.5676/DWD\_GPCC/FD\_D\_V2018\_100, 2018.
- Mawere, M.: Underdevelopment, Development and the Future of Africa, *Langaa Rpcig*, 2017.
- 35 McCabe, G. J., and Wolock, D. M.: Independent effects of temperature and precipitation on modeled runoff in the conterminous United States, *Water Resources Research*, 47, 2011.
- Messer, E., Cohen, M. J., and Marchione, T.: Conflict: A cause and effect of hunger, *Environmental Change and Security Project Report*, 7, 1-16, 2001.
- Mishra, S., Sahu, R., Eldho, T., and Jain, M.: An improved I a S relation incorporating antecedent moisture in SCS-CN methodology, *Water Resources Management*, 20, 643-660, 2006.
- 40 Mishra, S. K., and Singh, V. P.: A relook at NEH-4 curve number data and antecedent moisture condition criteria, *Hydrological Processes: An International Journal*, 20, 2755-2768, 2006.
- Moucha, R., and Forte, A. M.: Changes in African topography driven by mantle convection, *Nature Geoscience*, 4, 707, 2011.
- Murray-Tortarolo, G., Jaramillo, V. J., Maass, M., Friedlingstein, P., and Sitch, S.: The decreasing range between dry-and wet-season precipitation over land and its effect on vegetation primary productivity, *PLoS one*, 12, e0190304, 2017.
- 45 Ogden, F. L., Raj Pradhan, N., Downer, C. W., and Zahner, J. A.: Relative importance of impervious area, drainage density, width function, and subsurface storm drainage on flood runoff from an urbanized catchment, *Water Resources Research*, 47, 2011.
- Olang, L., and Fürst, J.: Effects of land cover change on flood peak discharges and runoff volumes: model estimates for the Nyando River Basin, Kenya, *Hydrological Processes*, 25, 80-89, 2011.
- Oyebande, L.: Water problems in Africa—how can the sciences help?, *Hydrological Sciences Journal*, 46, 947-962, 2001.
- 50 Paul, J. D., Roberts, G. G., and White, N.: The African landscape through space and time, *Tectonics*, 33, 898-935, 2014.
- Peel, M. C., Finlayson, B. L., and McMahon, T. A.: Updated world map of the Köppen-Geiger climate classification, *Hydrology and earth system sciences discussions*, 4, 439-473, 2007.
- Penman, J., Gytarsky, M., Hiraishi, T., Krug, T., Kruger, D., Pipatti, R., Buendia, L., Miwa, K., Ngara, T., and Tanabe, K.: Good practice guidance for land use, land-use change and forestry, *Good practice guidance for land use, land-use change and forestry*, 2003.
- 55 Ponce, V. M., and Hawkins, R. H.: Runoff curve number: Has it reached maturity?, *Journal of hydrologic engineering*, 1, 11-19, 1996.

- Ponette-González, A. G., Brauman, K. A., Marín-Spiotta, E., Farley, K. A., Weathers, K. C., Young, K. R., and Curran, L. M.: Managing water services in tropical regions: From land cover proxies to hydrologic fluxes, *Ambio*, 44, 367-375, 2015.
- Ruess, P.: Mapping of Water Stress Indicators, 2015.
- 5 Santhi, C., Arnold, J. G., Williams, J. R., Dugas, W. A., Srinivasan, R., and Hauck, L. M.: Validation of the swat model on a large rwer basin with point and nonpoint sources 1, *JAWRA Journal of the American Water Resources Association*, 37, 1169-1188, 2001.
- Save, H., Bettadpur, S., and Tapley, B. D.: High-resolution CSR GRACE RL05 mascons, *Journal of Geophysical Research: Solid Earth*, 121, 7547-7569, 2016.
- Sayre, and Pulley, A.: Africa, Twenty-First Century Books, 1999.
- 10 Schuol, J., Abbaspour, K. C., Yang, H., Srinivasan, R., and Zehnder, A. J.: Modeling blue and green water availability in Africa, *Water Resources Research*, 44, 2008.
- Shi, Z.-H., Chen, L.-D., Fang, N.-F., Qin, D.-F., and Cai, C.-F.: Research on the SCS-CN initial abstraction ratio using rainfall-runoff event analysis in the Three Gorges Area, China, *Catena*, 77, 1-7, 2009.
- Silveira, L., Charbonnier, F., and Genta, J.: The antecedent soil moisture condition of the curve number procedure, *Hydrological Sciences Journal*, 45, 3-12, 2000.
- 15 Smakhtin, V.: Taking into account environmental water requirements in global-scale water resources assessments, *Iwmi*, 2004.
- Sörensen, R., Zinko, U., and Seibert, J.: On the calculation of the topographic wetness index: evaluation of different methods based on field observations, *Hydrology and Earth System Sciences Discussions*, 10, 101-112, 2006.
- Sumarauw, J. S. F., and Ohgushi, K.: Analysis on curve number, land use and land cover changes and the impact to the peak flow in the Jobaru River Basin, Japan, *International Journal of Civil & Environmental Engineering IJCEE-IJENS*, 12, 17-23, 2012.
- 20 Terakawa, A.: Hydrological data management: Present state and trends, Secretariat of the World Meteorological Organization, 2003.
- Tesemma, Z. K., Mohamed, Y. A., and Steenhuis, T. S.: Trends in rainfall and runoff in the Blue Nile Basin: 1964–2003, *Hydrological processes*, 24, 3747-3758, 2010.
- United Nations, Department of Economic and Social Affairs, Population Division (2017). World Population Prospects: The 2017 Revision, Key Findings and Advance Tables, ESA/P/WP/248. <https://esa.un.org/unpd/wpp/Publications/>, 2017.
- 25 UNISDR: Global Assessment Report on Disaster Risk Reduction (GAR 2011). <https://www.preventionweb.net/english/hyogo/gar/>, 2011.
- UNISDR: Global Assessment Report on Disaster Risk Reduction (GAR 2015). <https://www.preventionweb.net/english/hyogo/gar/>, 2015.
- Urroz, G., Leines, R. C., Perret, G. L., Holland, J. M., and Hunsaker, B. E.: Development of a Low-cost, Self-calibrating Stream Gaging Station, 2001.
- 30 Van Liew, M., Arnold, J., and Garbrecht, J.: Hydrologic simulation on agricultural watersheds: Choosing between two models, *Transactions of the ASAE*, 46, 1539, 2003.
- Viessman Jr, W., and Knapp, J. W.: Introduction to hydrology, 1977.
- Walkenbach, J.: Excel 2010 power programming with VBA, John Wiley & Sons, 2010.
- Weng, Q.: Modeling urban growth effects on surface runoff with the integration of remote sensing and GIS, *Environmental management*, 28, 737-748, 2001.
- 35 Global Air Temperature and Precipitation Climatologies, by : Cort J. Willmott, Kenji Matsuura and David R. Legates (Center for Climate Research, University of Delaware), version 2.01, November 1998; <https://rda.ucar.edu/datasets/ds236.0/>, access: 15 January, 1998.
- Woodward, D. E., Hawkins, R. H., Jiang, R., Hjelmfelt, J., Allen T, Van Mullem, J. A., and Quan, Q. D.: Runoff curve number method: examination of the initial abstraction ratio, *World water & environmental resources congress 2003*, 2003, 1-10.
- 40 Wright, J. R., and Skiles, J.: SPUR Simulation of Production and Utilization of Rangelands: Documentation and User Guide, USDA-Agricultural Research Service, Northwest Watershed Research Center, 1987.
- Xiao, Y., Yi, S., and Tang, Z.: Integrated flood hazard assessment based on spatial ordered weighted averaging method considering spatial heterogeneity of risk preference, *Science of the Total Environment*, 599, 1034-1046, 2017.
- Yeo, I.-Y., Gordon, S. I., and Guldmann, J.-M.: Optimizing patterns of land use to reduce peak runoff flow and nonpoint source pollution with an integrated hydrological and land-use model, *Earth Interactions*, 8, 1-20, 2004.
- 45 Yuan, Y., Nie, W., McCutcheon, S. C., and Taguas, E. V.: Initial abstraction and curve numbers for semiarid watersheds in Southeastern Arizona, *Hydrological Processes*, 28, 774-783, 2014.
- Yuting, F., Yanning, C., Weihong, L., HuaiJun, W., and XinGong, L.: Impacts of temperature and precipitation on runoff in the Tarim River during the past 50 years, *干旱区科学*, 3, 220-230, 2011.
- Zeng, Z., Tang, G., Hong, Y., Zeng, C., and Yang, Y.: Development of an NRCS curve number global dataset using the latest geospatial remote sensing data for worldwide hydrologic applications, *Remote Sensing Letters*, 8, 528-536, 2017.
- 50 Zhu, X.: GIS for Environmental Applications: A practical approach, Routledge, 2016.



**Figure 16: The logo of Copernicus Publications.**